PCCP

Cite this: *Phys. Chem. Chem. Phys.*, 2012, **14**, 1014–1029

www.rsc.org/pccp

PAPER

Infrared spectrum of the 2-chloroethyl radical in solid *para*-hydrogen†

Jay C. Amicangelo,*[a] Barbara Golec,[b] Mohammed Bahou[b] and Yuan-Pern Lee*[bc]

Received 5th August 2011, Accepted 10th November 2011
DOI: 10.1039/c1cp22524c

The addition reaction of chlorine with ethylene (C_2H_4) is expected to proceed *via* a free radical intermediate, the 2-chloroethyl radical, however, this intermediate has not been previously observed spectroscopically. Irradiation at 365 nm of a co-deposited mixture of Cl_2, C_2H_4, and *p*-H_2 at 3.2 K produces a series of new lines in the infrared spectrum. A strong line at 664.0 cm^{-1} and weaker lines at 562.1, 1069.9, 1228.0, 3041.1 and 3129.3 cm^{-1} are concluded to be due to a single carrier based on their behavior upon subsequent annealing to 4.5 K and secondary irradiation at 254 and 214 nm. The positions and intensities of these lines agree with the MP2/aug-cc-pVDZ predicted vibrational spectrum of the 2-chloroethyl ($^{\bullet}CH_2CH_2Cl$) radical. In order to confirm this assignment, isotopic experiments were performed with C_2D_4 and *t*-$C_2H_2D_2$ and the corresponding infrared bands due to the deuterium isotopomers of this radical ($^{\bullet}CD_2CD_2Cl$ and $^{\bullet}C_2H_2D_2Cl$) have been observed. A final set of experiments were performed following irradiation of the $Cl_2/C_2H_4/p$-H_2 mixture at 365 nm, in which the matrix was irradiated with filtered infrared light from a globar source, which has been shown to induce reactions between isolated Cl atoms and matrix H_2 to produce HCl and H atoms. In these experiments, the major products observed were HCl, the ethyl radical ($^{\bullet}C_2H_5$) and ethyl chloride (C_2H_5Cl) and the possible mechanisms for the formation of these species are discussed.

1 Introduction

Understanding the reactions of chlorine atoms with hydrocarbons has relevance to several important applications and areas of research. In atmospheric chemistry, Cl atoms produced by the solar photodissociation of man-made chlorinated compounds, such as chlorofluorocarbons (CFCs), are known to contribute to the depletion of stratospheric ozone.[1–3] As well, it has also been proposed that Cl atoms may play an important role in the reactions of hydrocarbons in the troposphere, particularly the marine boundary layer[4,5] and the Arctic region.[6,7] The reactions of chlorine atoms with hydrocarbons are also of interest in understanding the processes involved in the incineration of hazardous wastes,[8–10] particularly chlorinated compounds and chemical weapons, and the industrial chlorination of organic compounds.[11]

From the chemical point of view, the reactions of chlorine and other chlorine containing molecules with unsaturated hydrocarbons and particularly alkenes are of interest because these are part of a fundamental class of reactions in organic chemistry, namely addition reactions.[12,13] The key feature in these types of reactions of alkenes is the ability of the alkene to undergo addition reactions with electrophiles, *e.g.* Cl_2, to the carbon–carbon double bond. When molecular chlorine reacts with alkenes in solution or the gas phase, the primary product is generally the dichloroalkane.[14,15] The reaction of chlorine atoms with alkenes has also been studied in the gas phase both experimentally[16–18] and theoretically.[19–22] In the gas phase reaction of Cl atoms with alkenes (C_nH_{2n}), the two most significant initial processes are the addition of a Cl atom to the carbon–carbon double bond to form a chloroalkyl radical ($^{\bullet}C_nH_{2n}Cl$), or the abstraction of a hydrogen atom to form an

[a] *School of Science, Penn State Erie, The Behrend College, 4205 College Drive, Erie, PA 16563, USA. E-mail: jca11@psu.edu*
[b] *Department of Applied Chemistry and Institute of Molecular Science, National Chiao Tung University, 1001 Ta-Hsueh Road, Hsinchu 30010, Taiwan. E-mail: yplee@mail.nctu.edu.tw*
[c] *Institute of Atomic and Molecular Sciences, Academia Sinica, Taipei 10617, Taiwan*

† Electronic supplementary information (ESI) available: B3LYP/aug-cc-pVDZ vibrational frequencies of the Cl + C_2H_4 addition and abstraction products (Table S1), MP2/aug-cc-pVDZ vibrational frequencies of the Cl_2–C_2H_4 complex and its isotopomers (Table S2), comparison of observed and calculated line positions and intensities of the Cl_2–C_2H_4 complex and its isotopomers (Table S3), MP2/aug-cc-pVDZ vibrational frequencies of 1,2-dichloroethane and its isotopomers (Table S4), comparison of observed and calculated line positions and intensities of 1,2-dichloroethane and its isotopomers (Table S5), MP2/aug-cc-pVDZ vibrational frequencies of ethyl chloride, CD_2HCD_2Cl isotopomers and C_2H_5 (Table S6), comparison of observed and calculated line positions and intensities of ethyl chloride and its isotopomers (Table S7), B3LYP/aug-cc-pVDZ structures of the Cl + C_2H_4 addition and abstraction products (Fig. S1), MP2/aug-cc-pVDZ structure of the Cl_2–C_2H_4 complex (Fig. S2), IR spectrum of 1,2-dichloroethane in *p*-H_2 (Fig. S3), structures of *gauche* and *trans* $C_2H_2D_2Cl_2$ (Fig. S4), MP2/aug-cc-pVDZ transition state structure for the reaction of the 2-chloroethyl radical with H_2 (Fig. S5), experimental IR difference spectra of a $Cl_2/C_2D_4/p$-H_2 matrix after 2 hours of irradiation at 365 nm followed by 2 hours of IR irradiation (Fig. S6), structures of the isotopomers of CD_2HCD_2Cl (Fig. S7), and a discussion of the results of the secondary IR irradiation experiments of $Cl_2/C_2D_4/p$-H_2 matrices. See DOI: 10.1039/c1cp22524c

alkyl radical ($^{\bullet}C_nH_{2n-1}$) and HCl, and the ratio of these two reactions has been observed to depend on alkene structure, pressure, and temperature.[16–18] The two radical products then react further to give stable molecular products, such as alkanes, monochloroalkanes, and dichloroalkanes.

Given the importance of chloroalkyl radicals in the mechanism of addition reactions of chlorine atoms with alkenes, direct spectral evidence of the existence of these species would be desirable. In this regard, the matrix isolation infrared (IR) absorption technique has proven to be a valuable method to produce and spectrally characterize radicals and other unstable species.[23,24] The use of the matrix isolation technique with conventional matrices (typically Ar or Ne) to study the reactions of Cl and other halogen atoms with small molecules has been somewhat limited due to the cage effect in which the Cl atoms produced by ultraviolet (UV) irradiation of Cl_2 cannot escape the original matrix cage and therefore most of the products observed involve the reaction of both Cl atoms.[25–27] The use of solid *para*-hydrogen (*p*-H_2) as a matrix has generated considerable interest in recent years[28,29] because it is considered as a quantum solid due to the fact that the amplitude of the zero-point lattice vibrations is a large fraction of the lattice spacing.[30,31] Therefore, solid *p*-H_2 is "softer" than noble gas matrices and this gives it several unique properties,[32–35] particularly a diminished cage effect,[36,37] which is relevant to the study of radical reactions, such as those of chlorine atoms with small molecules. In two recent studies, our group has demonstrated that co-deposition of Cl_2 with a reacting partner in *p*-H_2 followed by irradiation with UV light results in reaction products containing only a single chlorine atom.[38,39] In the first study, the reacting partner was CS_2 and the observed products were ClSCS, ClCS, and ClSC,[38] while in the second study the reacting partner was propylene (C_3H_6) and the observed product was the 2-chloropropyl radical ($^{\bullet}CH_2CHClCH_3$).[39]

To our knowledge, the latter study was the first report of the infrared spectrum of a chloroalkyl radical in the literature. Building on this previous work, in this paper we examined the reaction products resulting from the UV irradiation of co-deposited Cl_2 and C_2H_4 (or C_2D_4, *t*-$C_2H_2D_2$) in solid *p*-H_2 matrices using IR spectroscopy. In these experiments, we have observed a series of IR lines that we have assigned to the 2-chloroethyl radical ($^{\bullet}CH_2CH_2Cl$) or its isotopomers.

2 Experimental and computational methods

The details of the matrix isolation apparatus used in these experiments have been described previously.[35,38,40] All of the gases and chemicals used in these experiments were purchased from commercial suppliers and were used as received. Separate mixtures of C_2H_4, C_2D_4, or *trans*-$C_2H_2D_2$ in *p*-H_2 and Cl_2 in *p*-H_2 were co-deposited simultaneously onto a gold-plated copper block, which also served as a mirror to reflect the incident infrared beam to the detector, at 3.2 K (achieved with a Janis RDK-415 closed-cycle helium cryostat system) for 5–8 hours at equal rates of 7–8 mmol h^{-1}. The mixing ratio of the Cl_2/*p*-H_2 mixture was between 1 : 800 to 1 : 1000 and that of the C_2H_4/*p*-H_2 mixture was 1 : 1000. *p*-H_2 was produced by a low temperature conversion process in which normal H_2 gas was passed through a copper coil filled with a hydrated iron(III) oxide catalyst that was cooled with a closed-cycle helium refrigerator (Advanced Research Systems, DE204AF). The efficiency of the conversion was controlled by the temperature of the catalyst, which was typically 13–15 K in these experiments. At these temperatures, the concentration of *ortho*-hydrogen (*o*-H_2) was less than 100 ppm according to the Boltzmann distribution. Prior to entering the catalyst coil, the H_2 gas was passed through a trap cooled to 77 K before conversion to *p*-H_2. IR absorption spectra were recorded with a Bomem DA8 Fourier-transform IR spectrometer equipped with a KBr beamsplitter and a Hg/Cd/Te detector cooled to 77 K to cover the spectral range 500–5000 cm^{-1}. Typically 400 scans at 0.25 cm^{-1} resolution were co-added at each stage of the experiment.

To produce Cl atoms for reaction with C_2H_4, the Cl_2/C_2H_4/*p*-H_2 matrices were irradiated with 365 nm radiation from a light-emitting diode (Honle UV Technology, 375 mW) for 1–2 hours. The continuous emission from this source is superior to the emission from a pulsed laser, such as a frequency-tripled Nd : YAG laser at 355 nm, because the latter could easily boil off the *p*-H_2 matrix if too much power was employed. It has been previously reported that infrared (4000–5000 cm^{-1}) excitation of the solid *p*-H_2 can induce Cl atoms to react with *p*-H_2 to form HCl[41] and therefore when Cl atoms were present in the *p*-H_2 matrix, a 2.4 μm cutoff filter (Andover Corp.) was used when recording the IR spectra. Following the photolysis at 365 nm, the matrix was generally annealed to 4.5 K to induce diffusion for further reaction and for all matrices secondary photolysis was performed using a low-pressure Hg lamp (Pen-Ray lamp, UVP) with a 254 nm band pass filter (ESCO Products) and an unfiltered low-pressure Zn lamp to help distinguish the related product lines in the spectra. To also aid in the assignment of some of the IR product lines, an IR spectrum of 1 : 1000 1,2-dichloroethane in solid *p*-H_2 was obtained by depositing the mixture at 3.2 K for 10 minutes. In some experiments the effect of IR irradiation of the matrices after 365 nm photolysis was investigated and this was accomplished using a globar source with a filter passing 3870–4980 cm^{-1} (W02296-7, OCLI Products).

Quantum chemical calculations were used in this work to aid in the identification and interpretation of the IR spectra obtained. Geometry optimizations and vibrational frequency calculations were generally performed using Møller–Plesset second order perturbation theory (MP2)[42] with the aug-cc-pVDZ basis set[43] for the possible species that might be observed in these experiments. Some density functional theory calculations were also performed using the B3LYP hybrid functional[44–46] and the aug-cc-pVDZ basis set. All calculations used the Gaussian 03 suite of programs.[47] When vibrational frequencies calculated with MP2/aug-cc-pVDZ are compared with experimental frequencies, scaling factors of 0.978 and 0.949 are used for frequencies below and above 2000 cm^{-1}, respectively. For vibrational frequencies calculated with B3LYP/aug-cc-pVDZ, the corresponding scaling factors are 0.980 and 0.963, respectively. These values were obtained by determining the average deviations between the observed and calculated fundamental vibrational frequencies below and above 2000 cm^{-1} in the spectra of C_2H_4, C_2D_4 and *t*-$C_2H_2D_2$ in a *p*-H_2 matrix.

3 Results

3.1 Quantum chemical computations of Cl + C_2H_4 reaction products

3.1.1 Structures and vibrational frequencies of stationary points. The potential energy curves for the Cl + C_2H_4 addition and abstraction reactions have been previously studied by Sordo and coworkers at several levels of theory including the MP2/aug-cc-pVDZ level, however vibrational frequencies were not reported for the optimized stationary structures.[19] Therefore, the current quantum chemical calculations were performed in order to obtain theoretical IR spectra for the possible reaction products from the Cl + C_2H_4 reaction. The geometries and vibrational frequencies of the possible reaction products of Cl with C_2H_4 were computed at the MP2/aug-cc-pVDZ level of theory, which was shown to provide a reasonable description of the potential energy curves for the addition and abstraction reactions.[19] The targeted structures, which are displayed in Fig. 1, include several stationary points along the potential energy surface related to the chlorine atom addition reaction and the hydrogen atom abstraction reaction. The energy of each structure relative to the Cl + C_2H_4 reactants is also listed in Fig. 1 and is found to be in agreement with the values predicted by Sordo and co-workers.[19] The vibrational frequencies for the optimized structures are listed in Table 1. For several of the structures, the abbreviated nomenclature used in Fig. 1 and Table 1 is equivalent to that used by Sordo and co-workers.[19] Calculations were also performed at the B3LYP/aug-cc-pVDZ level, however, the B3LYP method does not predict that the I_{add} and I_{abs} complexes are stationary points along the potential energy curve, therefore B3LYP calculations were not performed on these structures. The optimized structures and vibrational frequencies for the four remaining species at the B3LYP/aug-cc-pVDZ level are given in the ESI† (Fig. S1, Table S1).

As can be seen from Fig. 1, the three structures related to the addition reaction pathway (I_{add}, $^{\bullet}CHClCH_3$, $^{\bullet}CH_2CH_2Cl$) are all predicted to be considerably stabilized with respect to the reactants and are therefore possible reaction products in our experiments. Based simply on the energies of the three structures I_{add}, $^{\bullet}CHClCH_3$, and $^{\bullet}CH_2CH_2Cl$, one might assume that since the 1-chloroethyl radical ($^{\bullet}CHClCH_3$) has the lowest energy of all three it might be the predominant species formed in the addition reaction of Cl with C_2H_4. However, Sordo and co-workers have shown that along the potential energy surface for the addition reaction, the reaction proceeds through the bridged species I_{add} followed by formation of the 2-chloroethyl radical ($^{\bullet}CH_2CH_2Cl$) in an exothermic and barrierless process. The 1-chloroethyl radical can be formed from the 2-chloroethyl radical by a 1,2 hydrogen shift, however, a significant barrier of

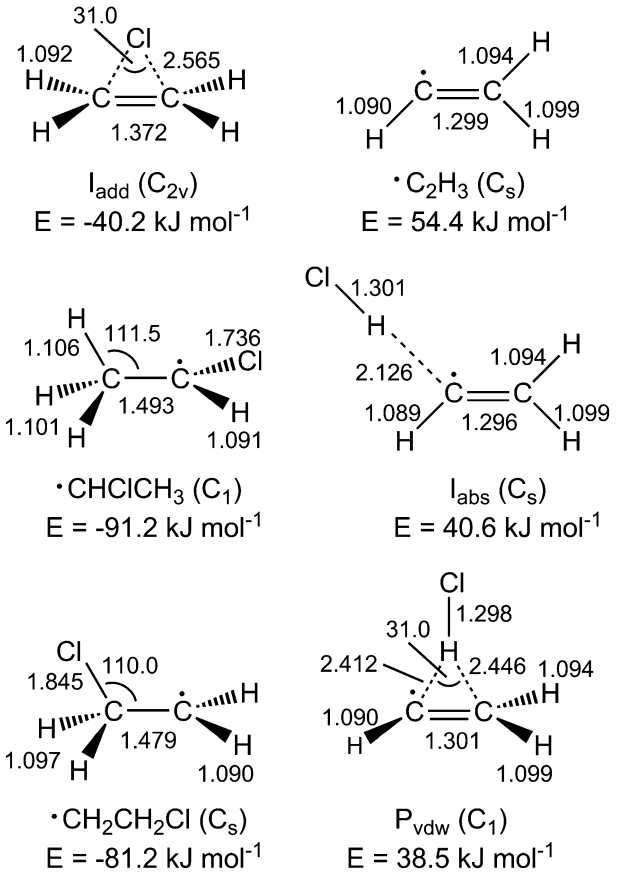

Fig. 1 Optimized geometries and energies (relative to the Cl + C_2H_4 reactants) at the MP2/aug-cc-pVDZ level for the intermediates and products of the addition and abstraction reactions between atomic chlorine and ethylene. For $^{\bullet}C_2H_3$, the relative energy includes the energy of HCl optimized at the same level of theory. The bond lengths are in angstroms and the bond angles are in degrees. The symmetry of each species is listed in parentheses. The 1-chloroethyl radical is listed as $^{\bullet}CHClCH_3$ and the 2-chloroethyl radical is listed as $^{\bullet}CH_2CH_2Cl$.

Table 1 Unscaled MP2/aug-cc-pVDZ calculated harmonic vibrational frequencies (cm^{-1}) and IR intensities (km mol^{-1}) of possible products of the addition and abstraction reactions between atomic chlorine and ethylene[a]

Species	Frequency (intensity)
I_{add}	240 (1.0), 351 (0.2), 616 (40.2), 825 (0.2), 976 (0.0), 1004 (62.9), 1228 (0.0), 1349 (8.8), 1448 (68.6), 1618 (20.0), 1976 (1843.2), 3202 (57.2), 3205 (3.0), 3299 (0.0), 3324 (0.2)
$^{\bullet}CHClCH_3$	182 (0.3), 336 (2.2), 471 (26.0), 744 (26.8), 998 (0.3), 1037 (18.2), 1133 (4.3), 1304 (39.9), 1393 (8.0), 1455 (8.7), 1470 (2.6), 3035 (14.6), 3125 (10.1), 3169 (8.2), 3255 (6.6)
$^{\bullet}CH_2CH_2Cl$	216 (1.5), 309 (12.0), 603 (3.0), 676 (95.3), 781 (0.8), 1070 (0.8), 1114 (9.2), 1256 (17.7), 1262 (0.3), 1466 (3.1), 1500 (0.1), 3132 (11.7), 3207 (1.6), 3209 (3.1), 3333 (2.6)
$^{\bullet}C_2H_3$	738 (16.9), 961 (24.7), 1058 (81.0), 1086 (9.3), 1412 (10.1), 1856 (4.0), 3143 (1.1), 3253 (1.5), 3297 (0.8)
I_{abs}	56 (0.7), 96 (4.0), 109 (7.9), 304 (11.7), 402 (18.4), 738 (14.3), 934 (31.8), 1069 (69.1), 1086 (7.5), 1412 (16.0), 1873 (3.2), 2801 (449.2), 3142 (0.2), 3251 (0.4), 3306 (4.1)
P_{vdw}	69 (1.4), 100 (0.6), 119 (12.0), 366 (8.2), 399 (11.0), 738 (16.8), 974 (27.3), 1071 (98.4), 1086 (11.4), 1413 (10.6), 1862 (12.1), 2866 (520.7), 3139 (0.2), 3249 (0.2), 3294 (1.7)

[a] The 1-chloroethyl radical is listed as $^{\bullet}CHClCH_3$ and the 2-chloroethyl radical is listed as $^{\bullet}CH_2CH_2Cl$.

approximately 180 kJ mol^{-1} is predicted at the MP2/aug-cc-pVDZ level,[19] which makes it unlikely that the 1-chloroethyl radical would be formed under our low temperature conditions. Therefore, the two most probable observable products of the addition reaction of a Cl atom with C_2H_4 are the bridged species I_{add} and the 2-chloroethyl radical. For the bridged species I_{add}, the predicted vibrational spectrum has the most intense line at 1976 cm^{-1} (CH_2 wag, unscaled), while for the 2-chloroethyl radical, the predicted vibrational spectrum has the most intense line at 676 cm^{-1} (CCl stretch/α-CH_2 out-of-plane bend, unscaled).

In contrast to the exothermic and barrierless nature of the addition reaction pathway, the three structures related to the abstraction pathway ($^{\bullet}C_2H_3$, I_{abs}, P_{vdw}) are all predicted to be higher in energy relative to the reactants. An initial barrier of approximately 43 kJ mol^{-1} is also predicted at the MP2/aug-cc-pVDZ level on the pathway from the reactants leading to I_{abs},[19] with this species then leading to the bridged species P_{vdw} and the HCl and $^{\bullet}C_2H_3$ products. Therefore, it seems unlikely that any of these three species would be formed under the current experimental conditions.

3.1.2 Vibrational frequencies of 2-chloroethyl radical isotopomers. As will be discussed below, in our experiments the only product observed involving the reaction of a single chlorine atom with C_2H_4 is the 2-chloroethyl radical ($^{\bullet}CH_2CH_2Cl$). Because experiments were also conducted with C_2D_4 and *trans*-$C_2H_2D_2$, vibrational frequency calculations at the MP2/aug-cc-pVDZ level were performed for the $^{\bullet}CD_2CD_2Cl$ and $^{\bullet}C_2H_2D_2Cl$ isotopomers and the unscaled frequencies are listed in Table 2.

For the mixed hydrogen–deuterium analogue of the 2-chloroethyl radical ($^{\bullet}C_2H_2D_2Cl$), six isotopomers are possible for this system, as displayed in Fig. 2. Structures I and II are enantiomers and can be classified as *s-trans* $^{\bullet}$CHDCHDCl; similarly structures III and IV are enantiomers and can be classified as *s-cis* $^{\bullet}$CHDCHDCl, and structures V and VI can be classified as geminal-D_2 $^{\bullet}CH_2CD_2Cl$ and $^{\bullet}CD_2CH_2Cl$. In terms of ZPE-corrected energies, structure V is predicted to be the lowest in energy, structures I–IV are all equivalent to each other and 1.2 kJ mol^{-1} higher than structure V, and structure VI is 2.3 kJ mol^{-1} higher than structure V. The resulting analysis of the vibrational frequencies for all of these isotopomers reveals that structures I and II have identical vibrational frequencies and structures III and IV have identical vibrational frequencies. Therefore, one would expect that these six isotopomers would give rise to only four sets of distinct vibrational frequencies: *s-trans* $^{\bullet}$CHDCHDCl (I and II), *s-cis* $^{\bullet}$CHDCHDCl (III and IV), $^{\bullet}CH_2CD_2Cl$ (V) and $^{\bullet}CD_2CH_2Cl$ (VI). Because our starting reagent in these experiments is the *trans*-$C_2H_2D_2$ isotopomer, it is expected that *s-trans* $^{\bullet}$CHDCHDCl would be the only product formed. However, Sordo and co-workers have calculated that the barrier to rotation about the C–C bond in the 2-chloroethyl radical is approximately 9 kJ mol^{-1} at the MP2/aug-cc-pVDZ level.[19] Since the formation of the 2-chloroethyl radical is predicted to be exothermic by −81 kJ mol^{-1} at the MP2/aug-cc-pVDZ level, the formation of *s-cis* $^{\bullet}$CHDCHDCl by rotation about the C–C bond might be accessible under our experimental conditions. Formation of $^{\bullet}CH_2CD_2Cl$ and $^{\bullet}CD_2CH_2Cl$ would require sequential 1,2 hydrogen and 1,2 deuterium shifts (or the reverse sequence) from $^{\bullet}$CHDCHDCl proceeding through the 1-chloroethyl radical as an intermediate. As described above in Section 3.1.1, the barrier height for inter-conversion between the 2-chloroethyl and 1-chloroethyl radicals *via* a 1,2 hydrogen shift is approximately 180 kJ mol^{-1}.[19] Therefore, it is unlikely that $^{\bullet}CH_2CD_2Cl$ and $^{\bullet}CD_2CH_2Cl$ isotopomers would be formed in our experiments and the most likely products would be the *s-trans* and *s-cis* isotopomers of $^{\bullet}$CHDCHDCl.

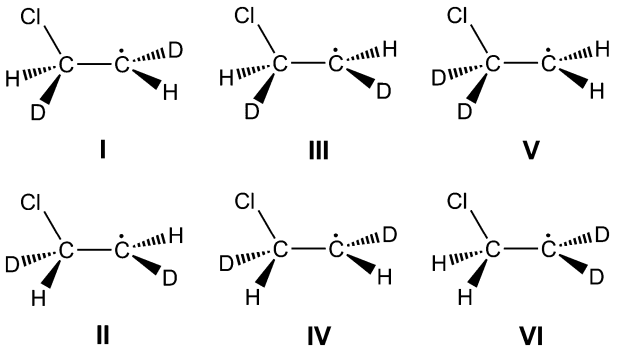

Fig. 2 Structures of the *s-trans* $^{\bullet}$CHDCHDCl (I/II), *s-cis* $^{\bullet}$CHDCHDCl (III/IV), $^{\bullet}CH_2CD_2Cl$ (V) and $^{\bullet}CD_2CH_2Cl$ (VI) isotopomers of the $^{\bullet}C_2H_2D_2Cl$ radical.

3.2 Deposition of $Cl_2/C_2H_4/p$-H_2, $Cl_2/C_2D_4/p$-H_2, and Cl_2/*trans*-$C_2D_2H_2/p$-H_2 matrices

The IR spectrum of C_2H_4 in *p*-H_2 at 3.2 K exhibits a number of intense and moderate lines at 3098.7 (ν_9), 2984.4, 2984.1 (ν_{11}),

Table 2 Unscaled MP2/aug-cc-pVDZ calculated harmonic vibrational frequencies (cm^{-1}) and IR intensities (km mol^{-1}) of the $^{\bullet}CD_2CD_2Cl$ radical and the isotopomers of the $^{\bullet}C_2H_2D_2Cl$ radical[a]

Species	Frequency (intensity)
$^{\bullet}CD_2CD_2Cl$	156 (1.1), 267 (10.9), 526 (7.0), 570 (0.2), 635 (60.8), 802 (0.1), 905 (3.9), 971 (23.5), 981 (0.3), 1084 (1.0), 1232 (8.2), 2275 (7.7), 2327 (0.9), 2385 (1.1), 2486 (1.8)
$^{\bullet}C_2H_2D_2Cl$	
I/II	178 (1.4), 296 (11.3), 570 (5.5), 641 (26.2), 654 (48.5), 860 (10.8), 950 (1.4), 1138 (15.6), 1224 (5.9), 1309 (2.2), 1384 (1.7), 2329 (4.9), 2400 (1.3), 3172 (6.2), 3277 (2.8)
III/IV	177 (1.4), 296 (11.4), 570 (5.2), 633 (7.7), 653 (69.1), 854 (6.5), 1008 (3.1), 1079 (11.5), 1226 (10.4), 1341 (2.6), 1365 (1.5), 2328 (4.8), 2401 (1.4), 3172 (6.3), 3277 (2.7)
V	215 (1.3), 306 (11.6), 598 (3.8), 650 (0.3), 661 (83.7), 816 (0.0), 923 (13.0), 1007 (14.7), 1122 (0.3), 1189 (8.6), 1487 (1.2), 2276 (7.6), 2386 (1.2), 3209 (3.1), 3332 (2.2)
VI	158 (1.3), 270 (11.2), 526 (6.9), 654 (0.4), 655 (70.4), 992 (5.6), 1009 (1.2), 1190 (3.8), 1218 (0.1), 1261 (19.6), 1480 (1.6), 2326 (1.1), 2486 (1.6), 3132 (11.7), 3208 (2.0)

[a] For the isotopomers of the $^{\bullet}C_2H_2D_2Cl$ radical, the roman numerals refer to the structures displayed in Fig. 2.

1440.0 (ν_{12}) and 948.6 (ν_7) cm^{-1} and a series of weaker lines at 3073.0 ($\nu_2 + \nu_{12}$), 2045.2, 2043.0 ($\nu_6 + \nu_{10}$), 1887.4 ($\nu_7 + \nu_8$), and 825.1, 824.4, 823.8, 823.0 (ν_{10}) cm^{-1}, in good agreement with the literature spectrum of C_2H_4.[48] With deposition of C_2D_4 in *p*-H_2 at 3.2 K, intense lines at 2339.0 (ν_9), 2199.1 (ν_{11}), 1075.0 (ν_{12}), and 720.1 (ν_7) cm^{-1} and weaker lines at 1495.5 ($\nu_7 + \nu_8$) and 595.6, 592.1 (ν_{10}) cm^{-1} are observed, in good agreement with the literature.[48] With deposition of *trans*-$C_2H_2D_2$ in *p*-H_2 at 3.2 K, intense lines at 3062.3, 3059.4 (ν_9), 2273.9, 2272.2 (ν_{11}), 1295.7 (ν_{12}), 987.0, 986.4, 986.1 (ν_4), and 725.2 (ν_7) cm^{-1} and weaker lines at 2303.0, 2302.3 ($\nu_6 + \nu_{12}$), 2222.5, 2220.3 ($\nu_2 + \nu_{10}$), 1953.5 ($\nu_3 + \nu_{10}$), 1844.4 ($\nu_4 + \nu_8$), and 672.8, 671.6 (ν_{10}) cm^{-1} are observed, in good agreement with the literature.[49]

Upon co-deposition of a mixture of Cl_2 in *p*-H_2 with C_2H_4 in *p*-H_2 at 3.2 K for several hours, a series of new lines or shoulders on the C_2H_4 lines are observed. These new lines are assigned to the Cl_2–C_2H_4 complex based on quantum chemical calculations performed at the MP2/aug-cc-pVDZ level of theory and by comparisons with previously reported vibrational frequencies for the Cl_2–C_2H_4 complex in low temperature nitrogen or argon matrices.[50,51] With co-deposition of Cl_2 with C_2D_4 or *trans*-$C_2H_2D_2$ in *p*-H_2 at 3.2 K, the analogous lines assigned to the Cl_2–C_2D_4 and Cl_2–*trans*-$C_2H_2D_2$ complexes, respectively, are observed and are found to be shifted as expected from the Cl_2–C_2H_4 complex lines. The predicted gas-phase structure of the Cl_2–C_2H_4 complex at the MP2/aug-cc-pVDZ level of theory, the full set of predicted vibrational frequencies for the Cl_2–C_2H_4, Cl_2–C_2D_4, and Cl_2–*trans*-$C_2H_2D_2$ complexes and the experimentally observed lines for the complexes are given in the ESI† (Fig. S2, Tables S2 and S3). Using the experimental intensities of several distinct lines for C_2H_4 and Cl_2–C_2H_4 and after accounting for the theoretical IR intensities of the lines, we estimate that the concentration ratio of C_2H_4 to Cl_2–C_2H_4 is (30 ± 10) : 1 in our experiments. It is worth noting that the quoted uncertainties in this concentration ratio and all others given below only represent the experimental fitting error and not the uncertainties in the theoretical IR intensities, which can be significant but are difficult to assess.

In addition to the lines of the Cl_2–C_2H_4, Cl_2–C_2D_4, and Cl_2–*trans*-$C_2H_2D_2$ complexes, weak lines of HCl (2894.2 and 2892.2 cm^{-1}) and the HCl–C_2H_4 (2772.7 and 2770.6 cm^{-1}), HCl–C_2D_4 (2770.0 and 2767.9 cm^{-1}), HCl–*trans*-$C_2H_2D_2$ (2771.3 and 2769.2 cm^{-1}) complexes are also observed in the co-deposition spectra.

3.3 Photolysis of $Cl_2/C_2H_4/p$-H_2 matrices

Upon photolysis of a deposited $Cl_2/C_2H_4/p$-H_2 mixture with 365 nm radiation a series of new IR lines appear, while the lines due to C_2H_4 and the Cl_2–C_2H_4 complex decrease in intensity. From an examination of the spectra before and after photolysis, it is estimated that ~7 ± 2% of C_2H_4 and ~48 ± 3% of Cl_2–C_2H_4 reacted during the photolysis. However, after correcting for the absolute intensities of the lines using the theoretical IR intensities, the concentration ratio of C_2H_4 to Cl_2–C_2H_4 reacted during photolysis is estimated to be (4 ± 2) : 1. Representative portions of the IR difference spectrum obtained by the subtraction of the co-deposited $Cl_2/C_2H_4/p$-H_2 spectrum from the spectrum after 2 hours of irradiation at 365 nm are presented in Fig. 3 trace (i). Lines pointing upwards indicate an increase in intensity and lines pointing downwards indicate a decrease in intensity.

3.3.1 Absorptions of 2-chloroethyl radical. As can be seen in Fig. 3 trace (i), the most prominent feature in the spectrum is a strong line at 664.0 cm^{-1}, which is a good candidate for the most intense vibrational mode of the 2-chloroethyl radical ($^{\bullet}CH_2CH_2Cl$) at 676 cm^{-1} predicted by theory (see Table 1). In order to help determine if any of the other new lines are associated with the 664.0 cm^{-1} line, a series of further consecutive experiments were performed on the 365 nm photolyzed sample: (1) annealing to 4.5 K for 30 minutes (trace (ii)), (2) irradiation at 3.2 K with a filtered Hg lamp at 254 nm for 2 hours (trace (iii)), (3) irradiation at 3.2 K with an unfiltered Zn lamp (most intense line is 214 nm) for 2 hours (trace (iv)), and annealing to 4.5 K for 30 minutes (trace (v)). All spectra were recorded with the matrix at 3.2 K and all spectra displayed in Fig. 3 traces (ii)–(v) are difference spectra obtained by subtraction of the spectrum recorded in the previous step from the current spectrum.

Upon annealing to 4.5 K, the line at 664.0 cm^{-1} was observed to increase while the lines of C_2H_4 are observed to decrease, suggesting that this line is due to a product of the reaction between Cl and C_2H_4 since some isolated Cl atoms would become mobile in the *p*-H_2 matrix at 4.5 K. In contrast to the 4.5 K annealing, when the matrix is subsequently irradiated using a filtered Hg lamp, the 664.0 cm^{-1} line decreases in intensity, trace (iii), and further irradiation using an unfiltered Zn lamp causes an additional decrease in intensity, trace (iv). Annealing the irradiated matrix again to 4.5 K results in an increase in the 664.0 cm^{-1} line, trace (v). Upon examining the behavior of the other new lines, it was determined that the medium intensity lines at 1069.9 and 1228.0 cm^{-1} and the weak lines at 562.1, 3041.1 and 3129.3 cm^{-1} are also observed to exhibit the same pattern of change with the additional annealing and photolysis experiments as the 664.0 cm^{-1} line and with nearly the same intensity ratio as the 664.0 cm^{-1} line as was observed in the spectrum in Fig. 3 trace (i). This suggests that these lines all belong to a common species, which we tentatively assign to the 2-chloroethyl radical ($^{\bullet}CH_2CH_2Cl$) based on a comparison with the predicted IR spectrum (see Table 1).

3.3.2 Absorptions of 1,2-dichloroethane. Of the remaining new lines displayed in Fig. 3 trace (i), the lines at 722.4, 725.0, 727.8 and 1232.0 cm^{-1} are assigned to the *trans* conformer of 1,2-dichloroethane ($C_2H_4Cl_2$) and the line at 1290.9 cm^{-1} is assigned to the *gauche* conformer of 1,2-dichloroethane based on a comparison with the literature vibrational frequencies for the two conformers,[52] the predicted vibrational spectra for the two conformers at the MP2/aug-cc-pVDZ level of theory, and a control experiment in which an authentic sample of 1,2-dichloroethane was deposited in a *p*-H_2 matrix at 3.2 K (Tables S4 and S5, Fig. S3 in ESI†). Using the experimental intensities of the 1290.9 and 1232.0 cm^{-1} lines and the corresponding theoretical vibrational frequencies and intensities, it is estimated that the concentration ratio of the *trans* to the

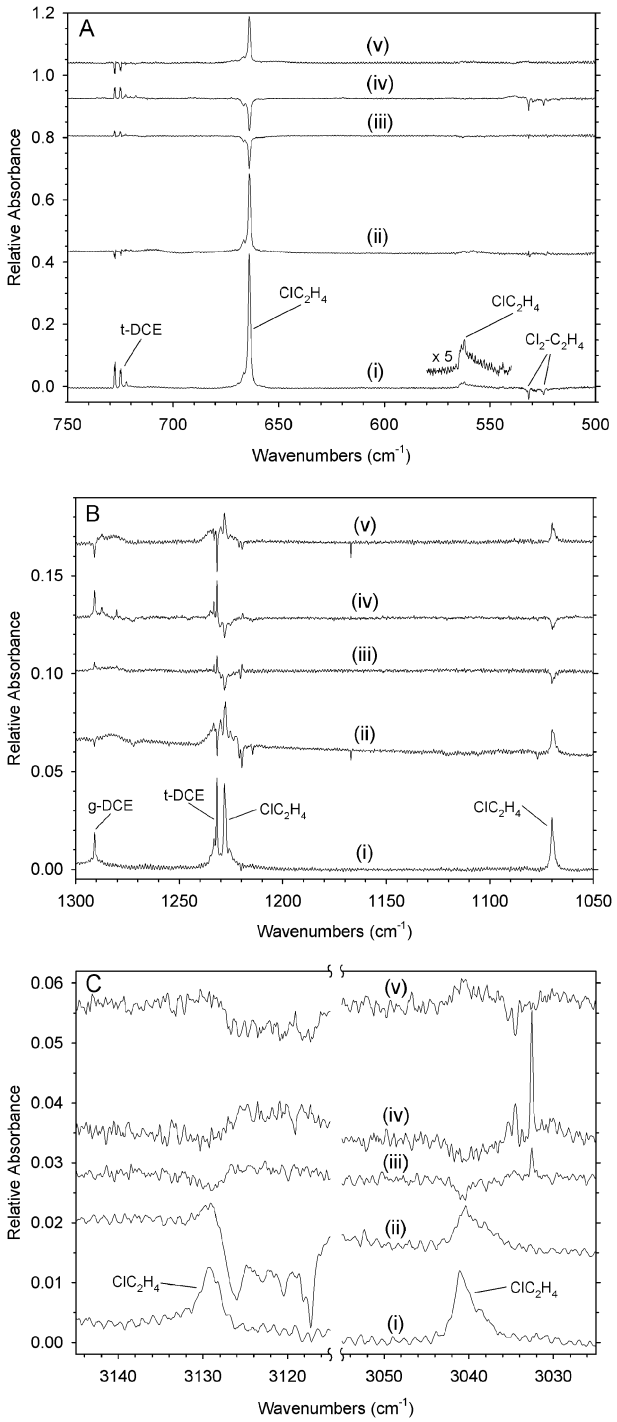

Fig. 3 Experimental IR difference spectra of an 8 hour co-deposited $Cl_2/C_2H_4/p\text{-}H_2$ (1 : 1 : 2000) matrix in the (A) 750–500 cm^{-1}, (B) 1300–1050 cm^{-1} and (C) 3145–3115 and 3055–3025 cm^{-1} regions (i) after 2 hours of irradiation at 365 nm at 3.2 K, (ii) after annealing of the matrix in (i) to 4.5 K for 30 minutes and recooling to 3.2 K, (iii) after 2 hours of irradiation of the matrix in (ii) using a filtered Hg lamp (254 nm) at 3.2 K, (iv) after 2 hours of irradiation of the matrix in (iii) using an unfiltered Zn lamp (predominately 214 nm) at 3.2 K, and (v) after annealing of the matrix in (iv) to 4.5 K for 30 minutes and recooling to 3.2 K. The spectra in traces (ii)–(v) have been offset for clarity. The lines assigned to *gauche* and *trans* 1,2-dichloroethane are labeled as *g*-DCE and *t*-DCE, respectively, and the lines assigned to the 2-chloroethyl radical are labeled as ClC_2H_4.

gauche conformer is (3.5 ± 0.2) : 1. When this analysis is applied to the authentic sample of 1,2-dichloroethane deposited in a $p\text{-}H_2$ matrix, it is found that the concentration ratio of the *trans* to the *gauche* conformer is (4.8 ± 0.2) : 1. Assuming that the *gauche* conformer is initially formed in the photolysis reaction (attack on the same side of the C_2H_4), the lower ratio observed in the photolysis *versus* the authentic sample deposition might indicate that internal rotation about the C–C bond is not completely free in the solid $p\text{-}H_2$ matrix, thereby reducing the amount of the *trans* conformer produced in the photolysis.

3.4 Photolysis of $Cl_2/C_2D_4/p\text{-}H_2$ matrices

Upon photolysis of a deposited $Cl_2/C_2D_4/p\text{-}H_2$ mixture with 365 nm radiation a series of new IR lines appear, while the lines due to C_2D_4 and the Cl_2–C_2D_4 complex decrease in intensity. A representative portion of the IR difference spectrum obtained by the subtraction of the co-deposited $Cl_2/C_2D_4/p\text{-}H_2$ spectrum from the spectrum after 2 hours of irradiation at 365 nm is presented in Fig. 4 trace (i).

3.4.1 Absorptions of deuterium 2-chloroethyl radical. A line at 592.4 cm^{-1} is the most prominent line observed in the 365 nm $Cl_2/C_2D_4/p\text{-}H_2$ photolysis experiment and is a good candidate to be the analogous deuterium line to the 664.0 cm^{-1} line observed in the $Cl_2/C_2H_4/p\text{-}H_2$ experiments. A similar set of experiments was performed, namely (1) annealing to 4.5 K for 30 minutes (trace (ii)), (2) irradiation at 254 nm with a filtered Hg lamp at 3.2 K for 3 hours (trace (iii)), (3) irradiation with an unfiltered Zn lamp (most intense line is 214 nm) at 3.2 K for 3 hours (trace iv)), and annealing to 4.5 K for 30 minutes (trace (v)).

By examining the behavior of the new lines in the $Cl_2/C_2D_4/p\text{-}H_2$ spectra, it was determined that the prominent line at 592.4 cm^{-1} and additional lines at 508.5, 892.2, 941.3, 1068.4, 1201.2, 2182.0, 2209.3, 2275.3, and 2362.4 cm^{-1} are also observed to exhibit the same pattern and nearly the same intensity ratio of change with the additional annealing and photolysis as was observed in the spectrum in Fig. 4 trace (i). There are three peaks on the low frequency side of the 592.4 cm^{-1} line (590.1, 588.2, 586.2 cm^{-1}), which display some changes in the relative intensity with the 592.4 cm^{-1} line upon annealing and secondary photolysis. We believe that these additional peaks are due to a combination of ^{37}Cl isotope splitting and matrix site splitting. The 941.3 cm^{-1} line is very close to a line of deuterated 1,2-dichloroethane at 940.4 cm^{-1} (see Section 3.4.2 below). However, because these two lines display opposite behavior upon additional annealing and photolysis, it is still clear that the 941.3 cm^{-1} line does exhibit the same pattern of change with additional annealing and photolysis as the other lines. Therefore, based on the annealing/photolysis behavior and a comparison with the predicted IR spectrum (see Table 2), the lines at 592.4, 892.2, 941.3, 1068.4, 1201.2, 2182.0, 2209.3, 2275.3, and 2362.4 cm^{-1} are tentatively assigned to the deuterium analogue of the 2-chloroethyl radical ($^{\bullet}CD_2CD_2Cl$).

3.4.2 Absorptions of deuterium 1,2-dichloroethane. By a comparison with the literature gas phase spectra of the *gauche* and *trans* conformers of deuterated 1,2-dichloroethane[52]

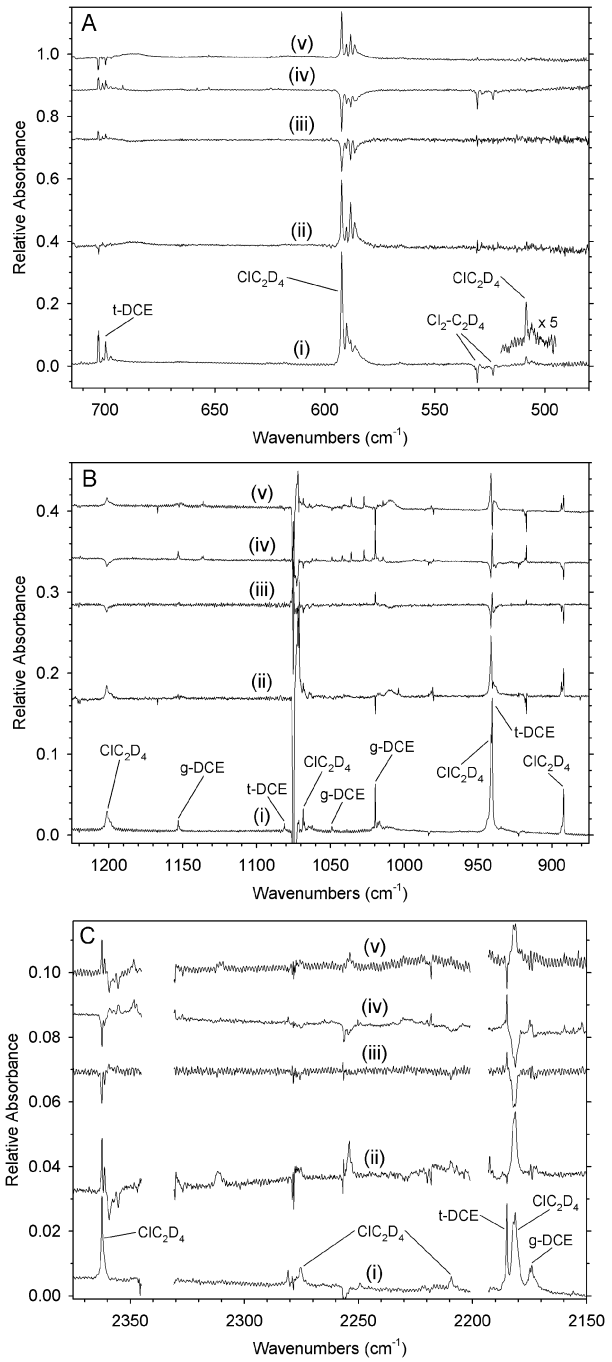

Fig. 4 Experimental IR difference spectra of an 8 hour co-deposited $Cl_2/C_2D_4/p\text{-}H_2$ (1 : 1 : 2000) matrix in the (A) 715–480 cm^{-1}, (B) 1225–875 cm^{-1} and (C) 2375–2150 cm^{-1} regions (i) after 2 hours of irradiation at 365 nm at 3.2 K, (ii) after annealing of the matrix in (i) to 4.5 K for 30 minutes and recooling to 3.2 K, (iii) after 3 hours of irradiation of the matrix in (ii) using a filtered Hg lamp (254 nm) at 3.2 K, (iv) after 3 hours of irradiation of the matrix in (iii) using an unfiltered Zn lamp (predominately 214 nm) at 3.2 K, and (v) after annealing of the matrix in (iv) to 4.5 K for 30 minutes and recooling to 3.2 K. In panel C, the spectral regions between 2345–2331 and 2201–2193 cm^{-1} have been removed due to the saturated lines of C_2D_4. The spectra in traces (ii)–(v) have been offset for clarity. The lines assigned to *gauche* and *trans* 1,2-dichloroethane are labeled as *g*-DCE and *t*-DCE, respectively, and the lines assigned to the 2-chloroethyl radical are labeled as ClC_2D_4.

and the MP2/aug-cc-pVDZ predicted vibrational spectra (Tables S4 and S5 in ESI†) of the two conformers, we are able to assign the lines at 697.3, 699.7, 702.8, 940.4, 1081.1 and 2184.9 cm^{-1} to the *trans* conformer and the lines at 1019.6, 1049.0, 1152.9, 2174.0 and 2174.8 cm^{-1} to the *gauche* conformer. Using the experimental intensities of the 1019.6 and 940.4 cm^{-1} lines and the corresponding theoretical vibrational frequencies and intensities, it is estimated that the concentration ratio of the *trans* to the *gauche* conformer is (4.5 ± 0.2) : 1.

3.5 Photolysis of $Cl_2/t\text{-}C_2H_2D_2/p\text{-}H_2$ matrices

Upon photolysis of a deposited $Cl_2/trans\text{-}C_2H_2D_2/p\text{-}H_2$ mixture with 365 nm radiation a series of new IR lines appear, while the lines due to *trans*-$C_2H_2D_2$ and the Cl_2–*trans*-$C_2H_2D_2$ complex decrease in intensity. Representative portions of the IR difference spectrum obtained by the subtraction of the co-deposited $Cl_2/trans\text{-}C_2H_2D_2/p\text{-}H_2$ spectrum from the spectrum after 3 hours of irradiation at 365 nm are presented in Fig. 5 trace (i).

3.5.1 Absorptions of mixed hydrogen–deuterium 2-chloroethyl radical. A pair of lines at 617.9 and 622.8 cm^{-1} are the most prominent of the new lines observed in the 365 nm $Cl_2/trans\text{-}C_2H_2D_2/p\text{-}H_2$ photolysis experiment. A similar set of experiments was performed, namely (1) annealing to 4.5 K for 30 minutes (trace (ii)), (2) irradiation with a filtered Hg lamp at 254 nm at 3.2 K for 4 hours (trace (iii)), and (3) irradiation with an unfiltered Zn lamp (most intense line is 214 nm) at 3.2 K for 2 hours (trace (iv)).

By comparing Fig. 3 with Fig. 5, the 617.9 and 622.8 cm^{-1} lines do exhibit similar changes to the 664.0 cm^{-1} line with additional annealing and photolysis. By examining the behavior of the new lines in the $Cl_2/trans\text{-}C_2H_2D_2/p\text{-}H_2$ spectra, it was determined that the prominent lines at 617.9 and 622.8 cm^{-1}, and additional lines at 537.4, 540.6, 643.6, 630.8, 840.2, 934.0, 1041.4, 1094.4, 1194.6, 1318.0, 2219.9, 2278.2, 2991.4, and 3085.6 cm^{-1} also exhibit the same pattern and nearly the same intensity ratio of change upon additional annealing and photolysis. Therefore, based on this and a comparison with the predicted IR spectra (Table 2), we tentatively assign these lines to mixed hydrogen–deuterium analogues of the 2-chloroethyl radical ($^{\bullet}C_2H_2D_2Cl$).

3.5.2 Absorptions of mixed hydrogen–deuterium 1,2-dichloroethane. Of the remaining new lines displayed in Fig. 5 trace (i), the lines at 713.0, 710.1, 707.3, 841.7, 870.6, 876.1, 892.8, 958.4, 966.0, 1054.2, 1067.1, 1187.9, 1221.0, 1232.9, 1249.8, 1255.1, 1302.3 and 1327.0 cm^{-1} are assigned to mixed hydrogen–deuterium 1,2-dichloroethane based on two factors: (1) a comparison of the behavior upon additional annealing and secondary photolysis with the behavior of the 1,2-dichloroethane lines in the $Cl_2/C_2H_4/p\text{-}H_2$ and $Cl_2/C_2D_4/p\text{-}H_2$ experiments and (2) a comparison with the MP2/aug-cc-pVDZ predicted vibrational spectra (Tables S4 and S5 in ESI†) of the mixed hydrogen–deuterium isotopomers of 1,2-dichloroethane ($C_2H_2D_2Cl_2$). Since the reactant (*trans*-$C_2H_2D_2$) has one hydrogen and one deuterium attached to each carbon atom, this arrangement is most likely preserved for $C_2H_2D_2Cl_2$. When one considers the possible configurations for the *trans* and *gauche* conformers of $C_2H_2D_2Cl_2$, there are actually four

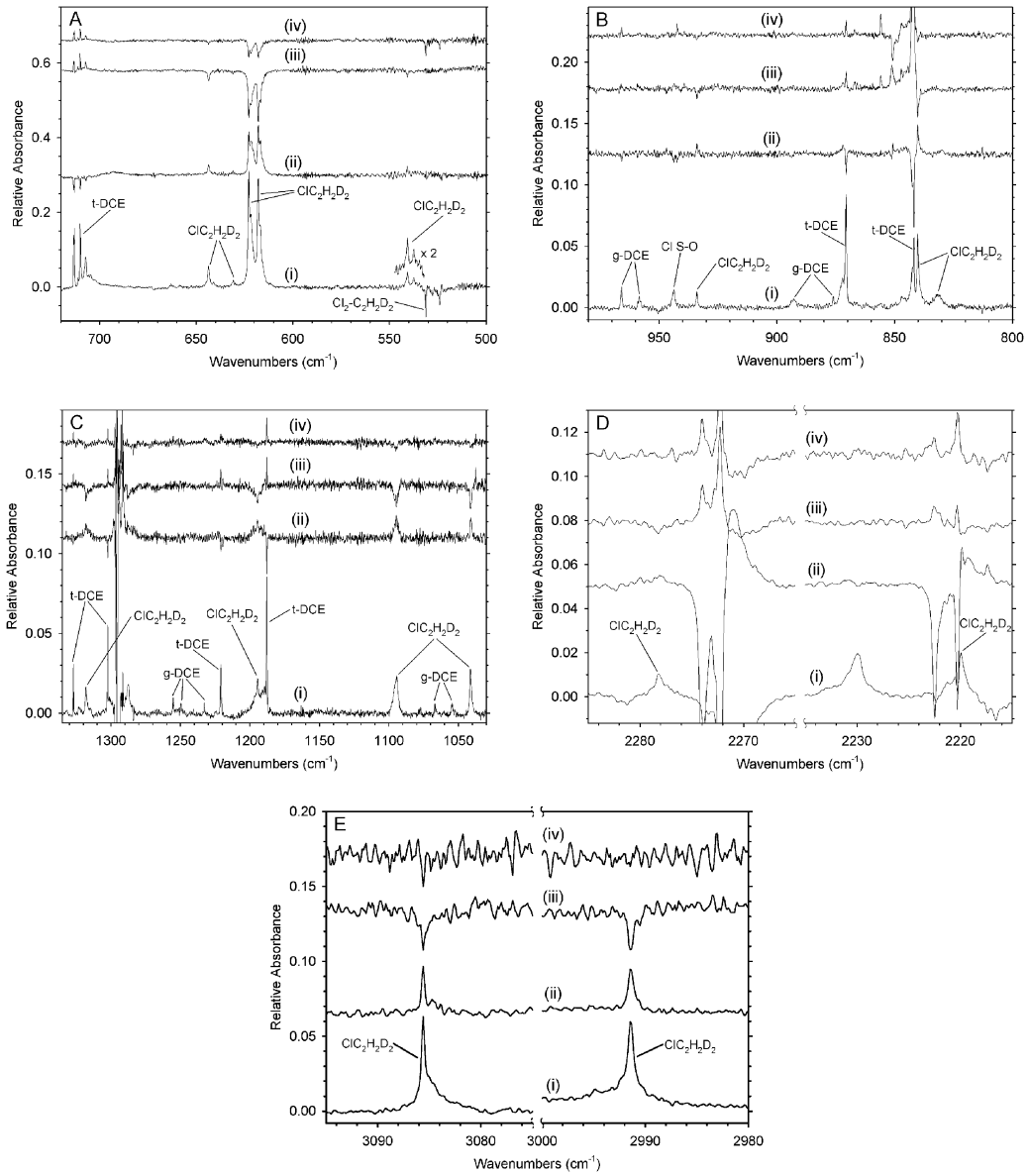

Fig. 5 Experimental IR difference spectra of a 7 hour co-deposited Cl_2/*trans*-$C_2H_2D_2$/*p*-H_2 (1 : 1 : 2000) matrix in the (A) 720–500 cm^{-1}, (B) 980–800 cm^{-1}, (C) 1335–1030 cm^{-1}, (D) 2285–2265 and 2235–2215 cm^{-1}, and (E) 3095–3075 and 3000–2980 cm^{-1} regions (i) after 3 hours of irradiation at 365 nm at 3.2 K, (ii) after annealing of the matrix in (i) to 4.5 K for 30 minutes and recooling to 3.2 K, (iii) after 4 hours of irradiation of the matrix in (ii) using a filtered Hg lamp (254 nm) at 3.2 K, and (iv) after 2 hours of irradiation of the matrix in (iii) using an unfiltered Zn lamp (predominately 214 nm) at 3.2 K. The spectra in traces (ii)–(iv) have been offset for clarity. The lines assigned to *gauche* and *trans* 1,2-dichloroethane are labeled as *g*-DCE and *t*-DCE, respectively, the line assigned to the Cl spin–orbit transition is labeled as Cl S–O and the lines assigned to the 2-chloroethyl radical are labeled as $ClC_2H_2D_2$.

trans isotopomers and four *gauche* isotopomers in which each carbon has one hydrogen and one deuterium atom attached to it (Fig. S4 in ESI†). The vibrational spectrum for each of these eight isotopomers was calculated at the MP2/aug-cc-pVDZ level and the full set of vibrational frequencies for each of these are listed in the ESI† (Table S4).

When the theoretical vibrational frequencies for the isotopomers are examined, it is determined that two distinct IR spectra are expected for the *trans* isotopomers and three distinct infrared spectra are expected for the *gauche* isotopomers. As a result of the moderate to large intensities of the experimental lines for the *trans* isotopomers, when the theoretical IR spectra for the two distinct *trans* isotopomers are compared to the spectrum in Fig. 5 trace (i), it is evident that lines due to both of the *trans* isotopomers are being observed. The lines at 841.7, 1221.0 and 1327.0 cm^{-1} are assigned to one of the *trans* isotopomers (*trans* B/C, Fig. S4 in ESI†) and the lines at 870.6, 1187.9 and 1302.3 are assigned to the other *trans* isotopomer (*trans* A/D, Fig. S4 in ESI†). The lines at 713.0, 710.1 and 707.3 cm^{-1} are due to overlapping lines of both *trans* isotopomers. Using the experimental intensities and corresponding theoretical intensities of several lines for the *trans* B/C and *trans* A/D isotopomers, it is estimated that the concentration ratio of the *trans* A/D to *trans* B/C isotopomers is (1.3 ± 0.2) : 1.

When the theoretical IR spectra for the three distinct *gauche* isotopomers are compared to the spectrum in Fig. 5 trace (i), the lines at 876.1, 892.8, 958.4, 966.0, 1054.2, 1067.1, 1232.9, 1249.8 and 1255.1 cm^{-1} were found to compare favorably with one or more of the *gauche* isotopomers and therefore these lines have been assigned as such. However, due to the weak intensities of these lines and the similarity of the predicted IR spectra for the three distinct *gauche* isotopomers, we are unable to assign these lines to specific *gauche* isotopomers. Therefore, we are also unable to determine the relative amount of each *gauche* isotopomer formed or to calculate an estimate of the total *trans* to *gauche* concentration ratio, but given the large intensities of the *trans* lines *versus* the *gauche* lines, it is clear that a larger amount of the *trans* 1,2-dichloroethane isotopomers are being formed.

3.6 Secondary IR irradiation of $Cl_2/C_2H_4/p$-H_2 matrices

Anderson and co-workers have recently shown that IR excitation (4000–5000 cm^{-1}) of matrices containing Cl atoms isolated in solid p-H_2 can induce the Cl atoms to react with p-H_2 to form HCl and H atoms and this is believed to occur by the creation of vibrationally excited $H_2(v = 1)$ which then possesses sufficient energy to react with the Cl atoms,[41,53]

$$Cl + H_2(v = 1) \rightarrow HCl + H. \quad (1)$$

Hence, secondary IR photolysis experiments were performed to further understand the reaction mechanism. The rationale for performing the secondary IR irradiation experiments is that if the 2-chloroethyl radical is being produced from the 365 nm irradiation, it might be induced to react with the mobile H atoms[54,55] produced in reaction (1) or to react directly with a vibrationally excited H_2 molecule.

$$^{\bullet}CH_2CH_2Cl + H \rightarrow C_2H_5Cl \quad (2)$$

$$^{\bullet}CH_2CH_2Cl + H_2(v = 1) \rightarrow C_2H_5Cl + H \quad (3)$$

Positive identification of ethyl chloride (C_2H_5Cl) would support the assignment of the 2-chloroethyl radical.

In the $Cl_2/C_2H_4/p$-H_2 experiment, the matrix was irradiated with 365 nm radiation for one hour followed by IR irradiation for two hours and several new, distinct lines appeared in the spectrum. The most intense of these correspond to the lines at (2894.1, 2892.2) cm^{-1} and (2772.7, 2770.6) cm^{-1}, which are due to the formation of HCl[56] and HCl–C_2H_4,[57] respectively. The spectral region that was found to be generally most informative regarding the additional products formed with IR irradiation is below 1500 cm^{-1} and representative portions of the IR difference spectrum in this region obtained by the subtraction of the 365 nm irradiated $Cl_2/C_2H_4/p$-H_2 spectrum from the spectrum after IR irradiation are presented in Fig. 6. By comparing the positions of the new lines observed in Fig. 6 with the literature IR spectrum[48] and the MP2/aug-cc-pVDZ predicted vibrational spectrum (Table S6) of ethyl chloride (C_2H_5Cl), the lines at 2938.1 (not shown), 1464.0, 1382.6, 1287.4, 1073.0, 972.0, 785.0 and 672.5 cm^{-1} are assigned to ethyl chloride. A table showing a direct comparison of the experimentally observed and MP2/aug-cc-pVDZ predicted vibrational frequencies and relative intensities for ethyl chloride is given in the ESI† (Table S7). The lines at

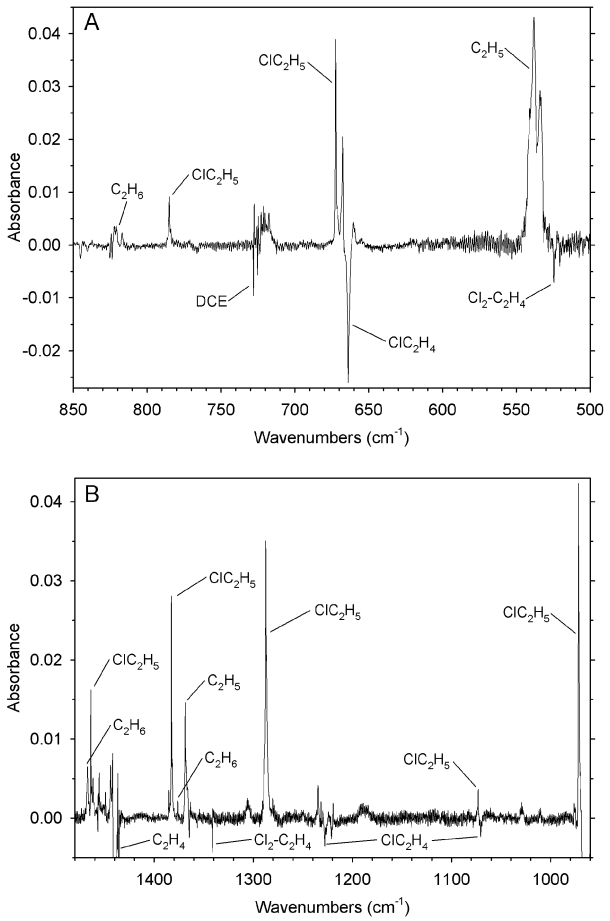

Fig. 6 Experimental IR difference spectra of an 8 hour co-deposited $Cl_2/C_2H_4/p$-H_2 (1 : 1 : 2000) matrix after 1 hour of irradiation at 365 nm at 3.2 K followed by 2 hours of IR irradiation (3876–4975 cm^{-1}) at 3.2 K in the (A) 900–500 cm^{-1} and (B) 1480–960 cm^{-1} regions. The lines assigned to the 2-chloroethyl radical and ethyl chloride are labeled as ClC_2H_4 and C_2H_5Cl, respectively.

3032.6 (not shown in Fig. 6), 1368.6, and 538.1 cm^{-1} are assigned to the $^{\bullet}C_2H_5$ radical based on comparisons with previous IR spectra in Ar and p-H_2 matrices[36,37,58,59] and the weak lines at 1467.1, 1376.2, 822.2 and 820.8 cm^{-1} are assigned to C_2H_6 based on a comparison with the literature gas phase spectrum.[48] Using the experimental intensities and the corresponding theoretical intensities of several lines of C_2H_5Cl and $^{\bullet}C_2H_5$, it is estimated that the concentration ratio of the $^{\bullet}C_2H_5$ to C_2H_5Cl is $(1.8 \pm 0.4) : 1$.

Secondary IR irradiation experiments were also performed with $Cl_2/C_2D_4/p$-H_2 matrices and the primary result was the observation of mixed hydrogen–deuterium isotopomers of ethyl chloride (CD_2HCD_2Cl). The information related to these experiments is given in the ESI† (Tables S6 and S7, Fig. S6 and S7, and Results section).

4 Discussion

4.1 Assignment of observed new lines to the 2-chloroethyl radical

In the $Cl_2/C_2H_4/p$-H_2 experiments, lines at 562.1, 664.0, 1069.9, 1228.0, 3041.1 and 3129.3 cm^{-1} were found to exhibit the same

Table 3 Comparison of observed experimental line positions (cm^{-1}) and relative intensities assigned to the 2-chloroethyl radical and its isotopomers in *p*-H_2 with the scaled harmonic vibrational frequencies and relative intensities calculated at the MP2/aug-cc-pVDZ level

Mode description[a]	ν_{expt}	I_{expt}[b]	ν_{MP2}[c]	I_{MP2}[d,e]
•CH_2CH_2Cl				
α-CH_2 antisym. stretch	3129.3	4.2	3163	2.7
α-CH_2 sym. stretch/β-CH_2 antisym. stretch	3041.1	6.0	3045/3043	3.2/1.7
β-CH_2 wag	1228.0	12.5	1228	18.6
CC stretch	1069.9	7.6	1089	9.7
CCl stretch/α-CH_2 OOP bend	664.0	100.0	661	100.0
α-CH_2 OOP bend	562.1	7.0	590	3.1
•CD_2CD_2Cl				
α-CD_2 antisym. stretch	2362.4	6.8	2359	3.0
β-CD_2 antisym. stretch	2275.3	2.4	2263	1.8
α-CD_2 sym. stretch	2209.3	1.0	2208	1.5
β-CD_2 sym. stretch	2181.2	11.9	2159	12.7
CC stretch/β-CD_2 scissor	1201.2	19.2	1205	13.5
β-CD_2 scissor/α-CD_2 scissor	1068.4	3.2	1060	1.6
β-CD_2 wag/α-CD_2 scissor	941.3	36.4	950	38.6
β-CD_2 wag	892.2	9.7	885	6.4
CCl stretch	592.4	100.0	621	100.0
α-CD_2 OOP bend	508.5	5.2	514	11.5
•CHDCHDCl				
s-cis/*s-trans* α-CH stretch	3085.6	12.3/11.8[f]	3110/3110	3.9/4.0
s-cis/*s-trans* β-CH stretch	2991.4	15.9/15.2[f]	3010/3010	9.1/9.0
s-cis/*s-trans* α-CD stretch	2278.2	2.7/2.6[f]	2279/2278	2.0/1.9
s-cis/*s-trans* β-CD stretch	2219.9	5.3/5.1[f]	2209/2210	6.9/7.1
s-cis α,β-CH wag	1318.0	7.4	1311	3.8
s-cis/*s-trans* β-CH wag	1194.6	16.4/16.1[f]	1199/1197	15.1/8.6
s-trans CC stretch	1094.4	25.5	1113	22.6
s-cis CC stretch	1041.4	14.2	1055	16.6
s-trans α,β-CD wag	934.0	2.6	929	2.0
s-trans β-CD wag	840.2	17.3	841	15.6
s-cis β-CD wag	831.6	8.6	835	9.4
s-trans α,β-CHD rock/CCl stretch	643.6	18.4	627	38.0
s-cis α,β-CHD rock/CCl stretch	630.8	4.8	619	11.1
s-trans CCl stretch/α,β-CHD rock	622.8	100.0	640	100.0
s-cis CCl stretch/α,β-CHD rock	617.9	100.0	639	100.0
s-trans α-CHD OOP bend	540.6	15.0	557	8.0
s-cis α-CHD OOP bend	537.4	9.2	557	7.5

[a] OOP indicates out-of-plane. [b] Intensities are normalized to the most intense line for each isotopomer. Experimental IR intensities are estimated by integrating the areas of the corresponding lines. For •CHDCHDCl, the lines assigned to the *s-cis* isotopomer are normalized to the line at 617.9 cm^{-1} and the lines assigned to the *s-trans* isotopomer are normalized to the line at 622.8 cm^{-1}. The experimental relative intensity of the 622.8 to the 617.9 cm^{-1} line is (1.04 ± 0.02) : 1. [c] The MP2/aug-cc-pVDZ calculated frequencies have been scaled by 0.978 and 0.949 for frequencies below and above 2000 cm^{-1}, respectively. [d] Intensities are normalized to the most intense predicted vibrational mode for each isotopomer. The MP2/aug-cc-pVDZ predicted intensity for the 661 cm^{-1} mode of •CH_2CH_2Cl is 95.3 km mol^{-1}, for the 621 cm^{-1} mode of •CD_2CD_2Cl is 60.8 km mol^{-1}, for the 639 cm^{-1} mode of *s-cis* •CHDCHDCl is 69.0 km mol^{-1}, and for the 640 cm^{-1} mode of *s-trans* •CHDCHDCl is 48.5 km mol^{-1}. [e] When two MP2 relative intensities are indicated, they correspond to the predicted frequencies listed in column 4. [f] These lines are assigned to both the *s-cis* and *s-trans* isotopomers of •CHDCHDCl. The two relative intensities listed result from normalization using the 617.9 cm^{-1} line (*s-cis*) or the 622.8 cm^{-1} line (*s-trans*), respectively.

behavior upon the additional annealing and photolysis experiments and it was concluded that these lines belong to a common species. When the experimental wavenumber and intensity pattern of these lines are compared with the MP2/aug-cc-pVDZ predicted vibrational frequencies and intensity patterns for all of the possible candidates listed in Table 1, the best agreement is found to be with the 2-chloroethyl radical (•CH_2CH_2Cl). The corresponding unscaled predicted frequencies are 603, 676, 1114, 1256, 3207/3209, and 3333 cm^{-1} and after scaling the predicted frequencies are 590, 661, 1089, 1228, 3043/3045, and 3163 cm^{-1}. Therefore, we assign the experimental IR lines listed above to the 2-chloroethyl radical, an expected intermediate in the reaction of Cl + C_2H_4. In the scaled MP2/aug-cc-pVDZ calculated vibrational frequencies for the 2-chloroethyl radical, there are lines predicted at 1434 and 2972 cm^{-1} that are expected to have observable intensities. We scrutinized our spectra in the regions of these predicted lines and were unable to find any experimental line that could be unambiguously assigned to the 2-chloroethyl radical. Most likely these lines are either obscured by the C_2H_4 and Cl_2–C_2H_4 lines near 2982–2986 cm^{-1} or their experimental intensities are lower than the predicted intensity and therefore unobservable in our experiments. The other expected lines of the 2-chloroethyl radical are most likely too weak to be observed in our experiments. In Table 3, the observed experimental line positions, along with the relative intensities, assigned to the 2-chloroethyl radical are compared with the scaled MP2/aug-cc-pVDZ predicted vibrational frequencies and relative intensities and as can be seen the agreement is very good, with frequency deviations between 0–5%. A visual comparison of the experimental spectrum to the scaled MP2/aug-cc-pVDZ predicted spectrum of •CH_2CH_2Cl is given in Fig. 7. Vibrational frequencies were also calculated for the 2-chloroethyl radical at

the B3LYP/aug-cc-pVDZ level (Table S1 in ESI†) and in general the agreement between the experimentally observed frequencies and relative intensities is good (lending additional support for the assignments), with most frequency deviations between 0–6% (scaled theoretical frequencies), however, there was a significant deviation for the lowest observed line (562.1 cm^{-1}) both in terms of frequency (19% deviation) and relative intensity (off by a factor of 20). Therefore, only the MP2/aug-cc-pVDZ calculated frequencies are presented in the following discussion.

In the $Cl_2/C_2D_4/p\text{-}H_2$ experiments, the lines at 508.5, 592.4, 892.2, 941.3, 1068.4, 1201.2, 2181.2, 2209.3, 2275.3, and 2362.4 cm^{-1} were found to exhibit the same behavior upon the additional annealing and photolysis experiments with each other and with those that have been assigned to the 2-chloroethyl radical in the $Cl_2/C_2H_4/p\text{-}H_2$ experiments. The experimental positions and intensities of these lines are found to compare very well with the scaled predicted vibrational frequencies and relative intensities for $^{\bullet}CD_2CD_2Cl$ at 514, 621, 885, 950, 1060, 1205, 2159, 2208, 2263, and 2359 cm^{-1}, strongly supporting the assignment of these lines to $^{\bullet}CD_2CD_2Cl$ (see Table 3 and Fig. 8). The other predicted lines of the deuterated 2-chloroethyl radical are most likely too weak to be observed in our experiments.

In the $Cl_2/trans\text{-}C_2H_2D_2/p\text{-}H_2$ experiments, the lines at 537.4, 540.6, 617.9, 622.8, 630.8, 643.6, 840.2, 934.0, 1041.4, 1094.4, 1194.6, 1318.0, 2219.9, 2278.2, 2991.4 and 3085.6 cm^{-1} were found to exhibit the same behavior upon the additional annealing and photolysis experiments with each other and with the lines assigned to the 2-chloroethyl radical in the $Cl_2/C_2H_4/p\text{-}H_2$ experiments. There are four isotopomers that are possible for this system depending on the relative orientation of H and D (Fig. 2), denoted as *s-trans* $^{\bullet}CHDCHDCl$, *s-cis* $^{\bullet}CHDCHDCl$, $^{\bullet}CH_2CD_2Cl$ and $^{\bullet}CD_2CH_2Cl$; based on energetic considerations only the *s-trans* $^{\bullet}CHDCHDCl$ and *s-cis* $^{\bullet}CHDCHDCl$ isotopomers are expected to be observable in our experiments.

By comparing the experimental line positions and intensities with the scaled calculated vibrational frequencies and intensities for the *s-trans* and *s-cis* $^{\bullet}CHDCHDCl$ isotopomers (see Table 3 and Fig. 9), the experimental lines at 537.4, 617.9, 630.8, 831.6, 1041.4, and 1318.0 cm^{-1} are found to compare favorably with the *s-cis* isotopomer and the experimental lines at 540.6, 622.8, 643.6, 840.2, 934.0, and 1094.4 cm^{-1} are found to compare favorably with the *s-trans* isotopomer. In the region below 1400 cm^{-1}, the *s-trans* and *s-cis* isotopomers both have a predicted line that is very close to each other at 1197 and 1199 cm^{-1}, respectively, and close to the 1194.6 cm^{-1} line. Therefore the 1194.6 cm^{-1} line is most likely due to overlapping lines of both isotopomers. In the C–D and C–H stretching regions, the lines for the *s-trans* and *s-cis* isotopomers are predicted to be very close to one another and most likely not resolvable. Therefore we assign the lines at 2219.9 and 2278.2 cm^{-1} as overlapping C–D stretching lines of the *s-trans* and *s-cis* isotopomers and the lines at 2991.4 and 3085.6 cm^{-1} as overlapping C–H stretching lines of the *s-trans* and *s-cis* isotopomers.

An estimate of the concentration ratio of the *s-trans* to the *s-cis* $^{\bullet}CHDCHDCl$ isotopomer in the initial 365 nm photolysis can be obtained by comparing experimental line areas for a *s-trans* and a *s-cis* line with the corresponding theoretical

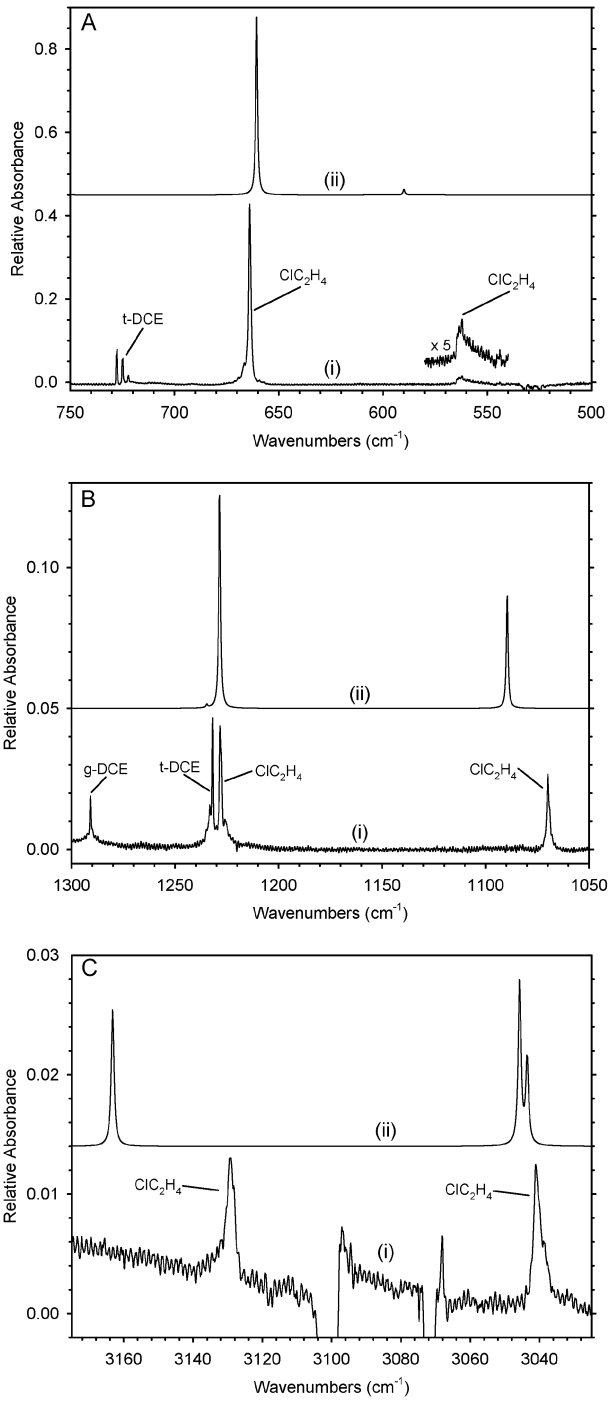

Fig. 7 Experimental IR difference spectra of an 8 hour co-deposited $Cl_2/C_2H_4/p\text{-}H_2$ (1 : 1 : 2000) matrix after 2 hours of irradiation at 365 nm at 3.2 K (i) and simulated harmonic infrared spectra for the $^{\bullet}CH_2CH_2Cl$ radical in the (A) 750–500 cm^{-1}, (B) 1300–1050 cm^{-1} and (C) 3175–3025 cm^{-1} regions. The simulated spectra are based on scaled harmonic vibrational frequencies computed at the MP2/aug-cc-pVDZ level of theory with a simulated half-width of 0.5 cm^{-1} and a resolution of 0.25 cm^{-1}. The intensities of the simulated spectra have been normalized such that the most intense vibrational mode was scaled to be equivalent to the experimental line at 664.0 cm^{-1}. The spectra in trace (ii) have been offset for clarity. The lines assigned to *gauche* and *trans* 1,2-dichloroethane are labeled as *g*-DCE and *t*-DCE, respectively, and the lines assigned to the 2-chloroethyl radical are labeled as ClC_2H_4.

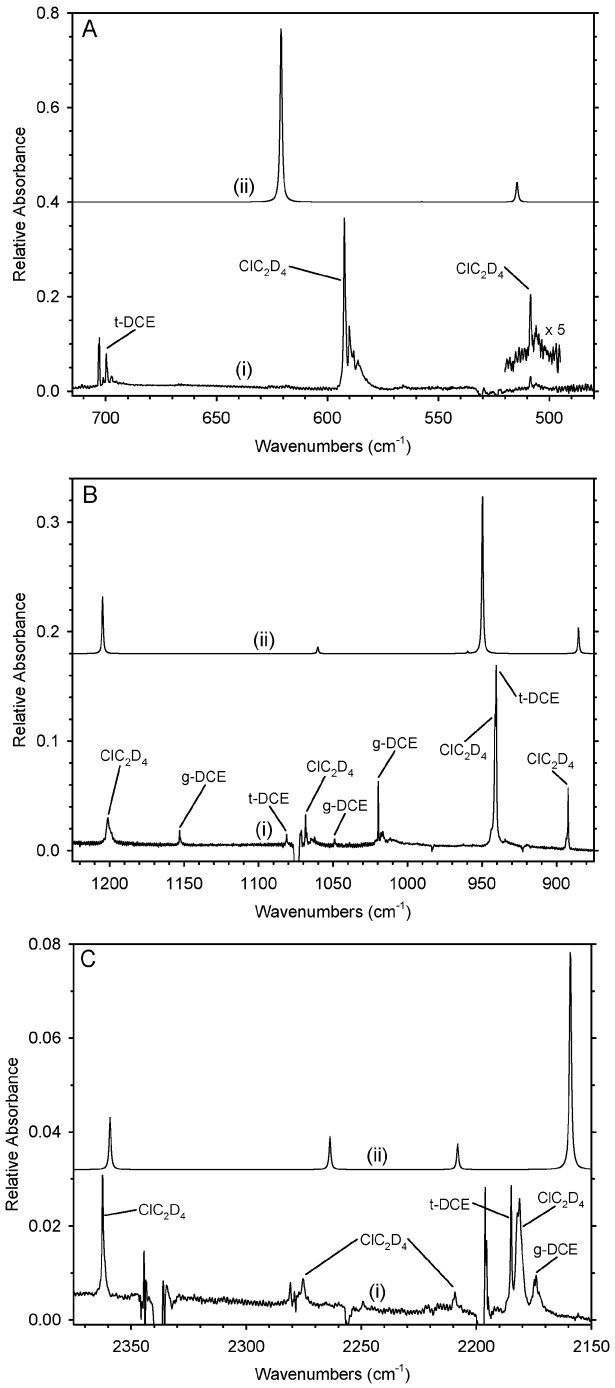

Fig. 8 Experimental IR difference spectra of an 8 hour co-deposited $Cl_2/C_2D_4/p$-H_2 (1 : 1 : 2000) matrix after 2 hours of irradiation at 365 nm at 3.2 K (i) and simulated harmonic infrared spectra for the $^{\bullet}CD_2CD_2Cl$ radical in the (A) 715–480 cm^{-1}, (B) 1225–875 cm^{-1} and (C) 2375–2150 cm^{-1} regions. The simulated spectra are based on scaled harmonic vibrational frequencies computed at the MP2/aug-cc-pVDZ level of theory with a simulated half-width of 0.5 cm^{-1} and a resolution of 0.25 cm^{-1}. The intensities of the simulated spectra have been normalized such that the most intense vibrational mode was scaled to be equivalent to the experimental line at 592.4 cm^{-1}. The spectra in trace (ii) have been offset for clarity. The lines assigned to *gauche* and *trans* 1,2-dichloroethane are labeled as *g*-DCE and *t*-DCE, respectively, and the lines assigned to the 2-chloroethyl radical are labeled as ClC_2D_4.

intensities. Using the experimental intensities of the 1094.4 and 1041.1 cm^{-1} lines and the corresponding theoretical vibrational frequencies and intensities it is estimated that the concentration ratio of the *s-trans* to the *s-cis* isotopomer in the initial 365 nm photolysis is (1.4 ± 0.1) : 1.

4.2 Formation of the 2-chloroethyl radical and diminished cage effect

Upon irradiation of a 3.2 K $Cl_2/C_2H_4/p$-H_2 matrix at 365 nm, the initial process is the dissociation of Cl_2 molecules to form Cl atoms. Photodissociation of gaseous Cl_2 at 365 nm could result in Cl atoms with 38 kJ mol^{-1} of translational energy.[41,53] Due to the high thermal conductivity of solid p-H_2 at 3.2 K,[31] this excess energy can be quickly dissipated and the Cl atoms effectively trapped in the p-H_2 matrix. Raston and Anderson have shown that the presence of Cl atoms isolated in a p-H_2 matrix can be confirmed by the observation of the weak $^2P_{1/2} \leftarrow {}^2P_{3/2}$ spin–orbit transition at 943.8 cm^{-1}.[60] In the experiments involving C_2H_4 and C_2D_4, the Cl spin–orbit transition was obscured by strong parent lines or strong lines from other products, however, for the experiments with *trans*-$C_2H_2D_2$ the Cl spin–orbit transition at 943.8 cm^{-1} was observed (Fig. 3B trace (i)), confirming the presence of some isolated Cl atoms in our p-H_2 matrices.

In addition to the Cl atoms just being stabilized and isolated in the p-H_2 matrix, if there are other molecules in the vicinity of the photo-produced Cl atoms, then the possibility of bimolecular reactions in the p-H_2 matrix exists. In the current experiments these molecules were C_2H_4 and their isotopomers C_2D_4 and *trans*-$C_2H_2D_2$. As described above, there are two main pathways by which a Cl atom can react with C_2H_4: H atom abstraction and Cl atom addition. The abstraction pathway is predicted to be endothermic (59 kJ mol^{-1}) and possesses a large barrier to reaction (52 kJ mol^{-1}). The addition pathway, in contrast, is predicted to be exothermic (−69 kJ mol^{-1}) and barrierless, proceeding through a symmetrical bridged intermediate (I_{add} in Fig. 1, −32 kJ mol^{-1}) on the way to the 2-chloroethyl radical structure ($^{\bullet}CH_2CH_2Cl$ in Fig. 1). A small barrier of 1 kJ mol^{-1} is predicted along the path from I_{add} to the 2-chloroethyl radical. The energies quoted above are from the QCISD(T)/aug-cc-pVDZ//MP2/aug-cc-pVDZ level of theory employed by Sordo and co-workers.[19]

In our experiments, the only products for the reaction of chlorine atoms with C_2H_4 observed upon 365 nm photolysis are the 2-chloroethyl radical and 1,2-dichloroethane. The Cl atom addition intermediate I_{add}, the 1-chloroethyl radical or any of the products of the abstraction reaction were not observed in the current experiments. Given that the initial barrier height for the hydrogen abstraction reaction is much higher than the upper limit of the translational energy of Cl, ~20 kJ mol^{-1} in the center-of-mass coordinate system, it is not surprising that none of the products of the abstraction reaction were observed in these experiments. The lack of observation of the I_{add} intermediate is consistent with the small barrier between I_{add} and the 2-chloroethyl radical and suggests that upon formation of I_{add}, the intermediate possesses sufficient energy to surmount the barrier and proceed directly to the 2-chloroethyl radical. The observation that the lines of the 2-chloroethyl radical increase with annealing to 4.5 K

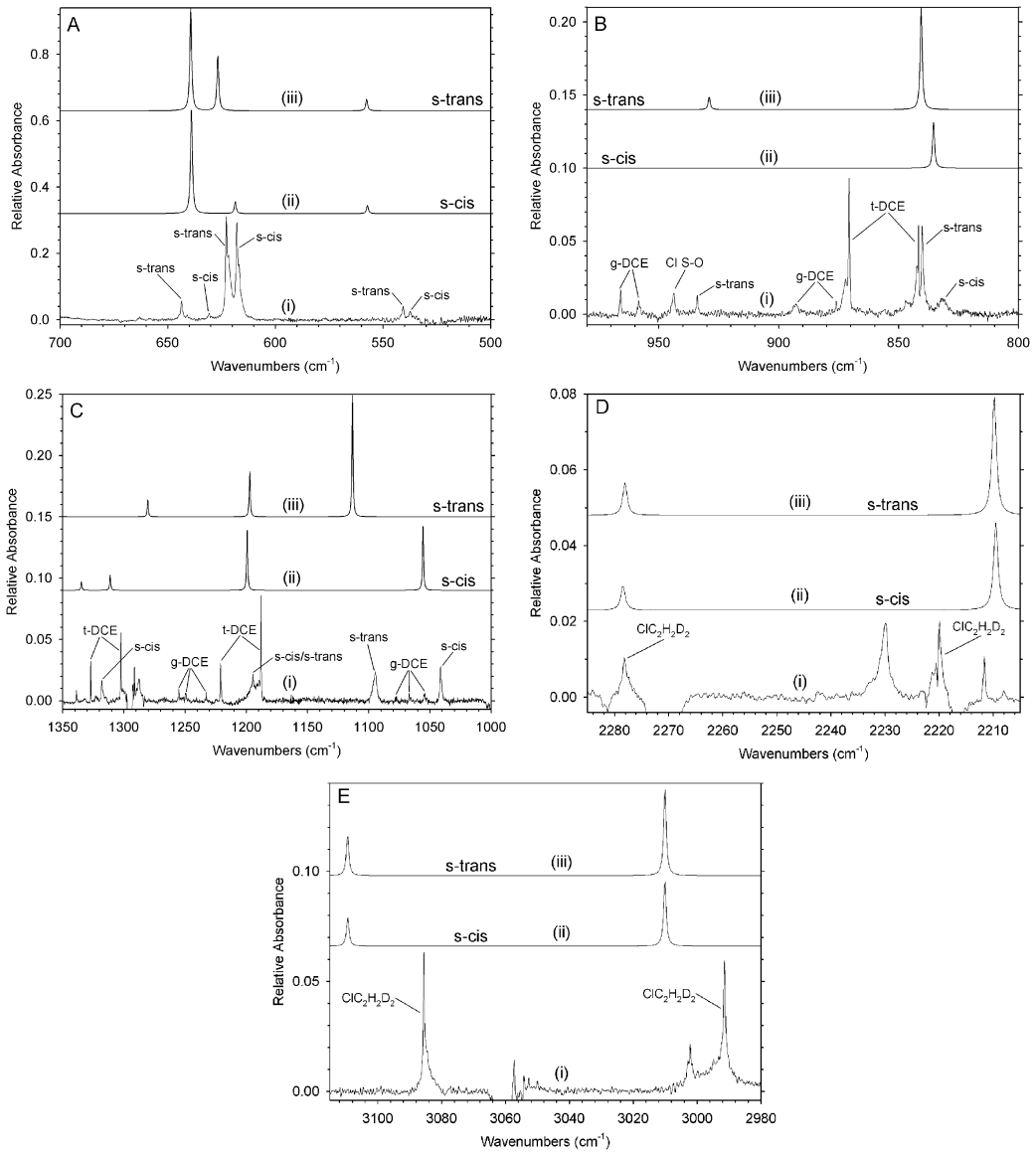

Fig. 9 Experimental IR difference spectra of a 7 hour co-deposited Cl_2/*trans*-$C_2H_2D_2$/*p*-H_2 (1 : 1 : 2000) matrix after 3 hours of irradiation at 365 nm at 3.2 K (i) and simulated harmonic infrared spectra for the *s-cis* (ii) and *s-trans* (iii) isotopomers of the •CHDCHDCl radical in the (A) 700–500 cm^{-1}, (B) 980–800 cm^{-1} (C) 1350–1000 cm^{-1}, (D) 2285–2205 cm^{-1} and (E) 3115–2980 cm^{-1} regions. The simulated spectra are based on scaled harmonic vibrational frequencies computed at the MP2/aug-cc-pVDZ level of theory with a simulated half-width of 0.5 cm^{-1} and a resolution of 0.25 cm^{-1}. The intensities of the simulated spectra have been normalized such that the most intense vibrational mode for each isotopomer was scaled to be equivalent to the experimental line at 622.8 cm^{-1}. The spectra in traces (ii)–(iii) have been offset for clarity. The lines assigned to *gauche* and *trans* 1,2-dichloroethane are labeled as *g*-DCE and *t*-DCE, respectively, the line assigned to the Cl spin–orbit transition is labeled as Cl S–O and the lines assigned to the *s-trans* and *s-cis* isotopomers of the •CHDCHDCl radical are labeled as *s-trans* and *s-cis*, respectively.

(essentially zero energy) supports the predicted barrierless nature of the Cl + C_2H_4 addition reaction. The fact that the 1-chloroethyl radical is not observed is also consistent with the large barrier for formation of the 1-chloroethyl radical from the 2-chloroethyl radical, which is too large to be overcome under the current experimental conditions. The formation of both the *s-trans* and *s-cis* isotopomers of •CHDCHDCl with an estimated concentration ratio of (1.4 ± 0.1) : 1 in the Cl_2/*trans*-$C_2H_2D_2$/*p*-H_2 experiments is consistent with the predicted low barrier to rotation about the C–C bond (9 kJ mol^{-1}), suggesting that the 2-chloroethyl radical is sufficiently excited upon formation and can proceed over the barrier, resulting in the formation of the *s-cis* isotopomer from the initially formed *s-trans* isotopomer.

The formation of 1,2-dichloroethane presumably occurs from the addition of a second Cl atom to the 2-chloroethyl radical. Sordo and co-workers[19] did not characterize this secondary Cl addition pathway in their study of the reaction of Cl with C_2H_4, but Kurosaki[61] did calculate the energetics of this pathway and reported that the addition of a second Cl atom to the 2-chloroethyl radical to form 1,2-dichloroethane is barrierless and has an exothermicity of 332 or 326 kJ mol^{-1} at

the MP2/6-31+G(d,p) level of theory depending on whether the product is *trans* or *gauche* 1,2-dichloroethane, respectively. In our own calculations at the MP2/aug-cc-pVDZ level, the exothermicity is found be 336 or 329 kJ mol^{-1}, respectively. Therefore, it is not surprising that 1,2-dichloroethane is formed as a product in our 365 nm photolysis experiments.

The observation of 2-chloroethyl radical demonstrates a very unique feature of solid *p*-H_2 as a low temperature matrix material as compared to noble gas matrices. The diminished cage effect for solid *p*-H_2 allows one of the Cl atoms to escape the matrix cage after photolysis, allowing only one Cl atom to react with the C_2H_4 rather than both Cl atoms reacting with C_2H_4. This is generally not the case when similar *in situ* photolysis experiments involving dihalogen molecules have been performed in low temperature noble gas matrices, in which the major products observed typically included both halogen atoms due to the cage effect.[25–27]

4.3 Reactions during secondary IR irradiation

Upon secondary IR irradiation of a $Cl_2/C_2H_4/p$-H_2 matrix at 3.2 K that had been previously irradiated at 365 nm, the most intense lines are due to HCl and the HCl–C_2H_4 complex. The HCl is being formed by reaction (1) and has been shown to readily occur upon IR irradiation of a *p*-H_2 matrix containing Cl atoms.[41,53] The observation of HCl–C_2H_4 indicates that some of the HCl is produced in the vicinity of C_2H_4 and subsequently forms a complex with C_2H_4. Of the remaining lines, the two major products are found to be ethyl chloride (C_2H_5Cl) and the ethyl radical ($^{\bullet}C_2H_5$) and a minor product being ethane (C_2H_6). The formation of HCl by reaction (1) implies that H atoms are being formed in the *p*-H_2 matrix and H atoms are thought to be very mobile in solid *p*-H_2 even at 3.2 K.[54,55] Therefore, the most direct pathway to form ethyl chloride is the reaction of H atoms with the 2-chloroethyl radical (reaction (2)), which is predicted to be exothermic by 394 kJ mol^{-1} at the MP2/aug-cc-pVDZ level and should be a barrierless reaction. The most direct pathway to form the ethyl radical is the reaction of H atoms with ethylene (reaction (4)), which has an experimental exothermicity of 151 kJ mol^{-1} [62] and has a small barrier of approximately 6 kJ mol^{-1} in the gas phase.[63]

$$C_2H_4 + H \rightarrow {}^{\bullet}C_2H_5 \quad (4)$$

The fact that the ethyl radical is observed suggests that the H atoms formed in reaction (1) either have enough residual energy to surmount the barrier or they react with the C_2H_4 *via* a tunneling mechanism. Ethane is most likely being formed by the reaction of H atoms with the ethyl radical (reaction (5)) which is a barrierless reaction that has an experimental exothermicity of 421 kJ mol^{-1}.[62]

$$^{\bullet}C_2H_5 + H \rightarrow C_2H_6 \quad (5)$$

In addition to the reaction of the 2-chloroethyl radical with H atoms (reaction (2)), it is also possible that the 2-chloroethyl radical can react directly with a vibrationally excited H_2 molecule to form ethyl chloride (reaction (3)). The reaction of the 2-chloroethyl radical with a vibrationally ground state H_2 molecule ($v = 0$) is predicted to have an exothermicity of 7 kJ mol^{-1} at the MP2/aug-cc-pVDZ level. The fact that the 2-chloroethyl radical can be stabilized in solid *p*-H_2 suggests that there is a barrier to the ground state reaction. To investigate this, quantum chemical calculations were performed at the MP2/aug-cc-pVDZ level to find the transition state for reaction (3) with the H_2 molecule in its vibrational ground state. The transition state structure that was obtained (Fig. S5 in ESI†) was found to possess one negative frequency corresponding to the motion of the inner hydrogen of H_2 toward the carbon radical, therefore this is the transition state connecting the 2-chloroethyl radical and H_2 reactants with the ethyl chloride and H atom products. This structure is predicted to be 47 kJ mol^{-1} higher in energy than the 2-chloroethyl radical and H_2 reactants. The pure vibrational transition (Q1(0); $v = 1, j = 0 \leftarrow v = 0, j = 0$) of solid *p*-$H_2$ has been observed near 4150 cm^{-1} (50 kJ mol^{-1}) for Cl_2 doped solid *p*-H_2 matrices.[41] Taking this as an estimate of the energy available for reaction with a vibrationally excited H_2, it seems feasible that some fraction of the 2-chloroethyl radicals might be reacting directly with vibrationally excited H_2 (reaction (3)) as well as reacting with H atoms (reaction (2)). Experimentally it is not possible to determine the exact relative amount of reaction (2) *versus* reaction (3) occurring because the observable species in both reactions are identical.

To determine if the 2-chloroethyl radical is the primary reactant to produce ethyl chloride, the concentration ratio of ethyl chloride produced to the 2-chloroethyl radical consumed was calculated using experimental and theoretical intensities of various lines for each molecule and was found to be $(5 \pm 1) : 1$. This suggests that the 2-chloroethyl radical is not the sole reactant for the production of ethyl chloride. Two other possible reactions to produce ethyl chloride are the reactions of the ethyl radical with Cl atoms (reaction (6)) or Cl_2 molecules (reaction (7)), which have experimental exothermicities of 349 and 107 kJ mol^{-1}, respectively.[62]

$$^{\bullet}C_2H_5 + Cl \rightarrow C_2H_5Cl \quad (6)$$

$$^{\bullet}C_2H_5 + Cl_2 \rightarrow C_2H_5Cl + Cl \quad (7)$$

Of these two reactions, reaction (6) does not have a barrier, whereas reaction (7) has a barrier of approximately 4 kJ mol^{-1} in the gas phase.[63] From Fig. 6, it is clear that the Cl_2–C_2H_4 complex is also reacting upon IR irradiation and a third possible additional reaction to form ethyl chloride is the reaction of the Cl_2–C_2H_4 complex with H atoms (reaction (8)) in a two step process that could involve the initial formation of the Cl_2–$^{\bullet}C_2H_5$ complex and then internal reaction of $^{\bullet}C_2H_5$ with Cl_2, for which the overall process is predicted to have an exothermicity of 267 kJ mol^{-1} at the MP2/aug-cc-pVDZ level.

$$Cl_2\text{–}C_2H_4 + H \rightarrow Cl_2\text{–}{}^{\bullet}C_2H_5 \rightarrow C_2H_5Cl + Cl \quad (8)$$

Because the second step of this process is essentially equivalent to reaction (7), reaction (8) would be expected to have a barrier of similar magnitude, *i.e.* approximately 4 kJ mol^{-1}.

5 Conclusions

The reaction of chlorine atoms with ethylene (C_2H_4) and two of its deuterium isotopomers (C_2D_4 and *t*-$C_2H_2D_2$) in solid

para-hydrogen (p-H_2) matrices at 3.2 K has been studied using infrared spectroscopy. Irradiation at 365 nm of a co-deposited mixture of Cl_2, C_2H_4, and p-H_2 at 3.2 K produces a series of new lines in the infrared spectrum. An intense line at 664.0 cm^{-1} and weaker lines at 562.1, 1069.9, 1228.0, 3041.1 and 3129.3 cm^{-1} are concluded to be due to a single carrier based on their behavior upon subsequent annealing to 4.5 K and secondary irradiation at 254 and 214 nm. When the positions and intensities of these lines are compared to the MP2/aug-cc-pVDZ predicted vibrational spectra of the possible species that could result from the addition and abstraction reactions of one Cl atom with C_2H_4, we assign these lines to absorption of the 2-chloroethyl radical ($^{\bullet}CH_2CH_2Cl$). Isotopic experiments were also performed with C_2D_4 and t-$C_2H_2D_2$ and the corresponding infrared bands due to the deuterium isotopomers of this radical ($^{\bullet}CD_2CD_2Cl$ and $^{\bullet}C_2H_2D_2Cl$) have been observed, confirming the assignment of the 2-chloroethyl radical. The other major species observed in the 365 nm irradiation experiments are the *gauche* and *trans* conformers of 1,2-dichloroethane ($C_2H_4Cl_2$) resulting from the addition of two Cl atoms to C_2H_4. The fact that the 2-chloroethyl radical can be observed in these experiments demonstrates one of the unique features of solid p-H_2 as a low temperature matrix, namely a diminished cage effect that allows for the reaction of a single Cl atom after photolysis of Cl_2 in the matrix rather than only reaction of both Cl atoms as often occurs in low temperature rare gas matrices.

An additional set of experiments was performed following irradiation of the $Cl_2/C_2H_4/p$-H_2 mixture at 365 nm, in which the matrix was irradiated with filtered infrared light from a globar source (3870–4980 cm^{-1}), which has been shown to induce a reaction between isolated Cl atoms and matrix H_2 to produce HCl and H atoms.[41,53] The major products observed were HCl, the ethyl radical ($^{\bullet}C_2H_5$) and ethyl chloride (C_2H_5Cl). The ethyl radical is formed by the addition reaction of H atoms with C_2H_4. Ethyl chloride is believed to be formed from several reactions involving the 2-chloroethyl radical with H atoms or H_2, the ethyl radical with Cl atoms or Cl_2, and the Cl_2–C_2H_4 complex with H atoms.

Acknowledgements

This work was supported by the National Science Council of Taiwan grant NSC99-2745-M-009-001-ASP. J. A. also acknowledges support in the form of a Fulbright Research Grant from the Foundation for Scholarly Exchange (Fulbright Taiwan) and the J. William Fulbright Foreign Scholarship Board (U. S. State Department).

References

1 S. F. Rowland, *Annu. Rev. Phys. Chem.*, 1991, **42**, 731–768.
2 M. J. Molina, L. T. Molina and C. E. Kolb, *Annu. Rev. Phys. Chem.*, 1996, **47**, 327–367.
3 B. J. Finlayson-Pitts and J. N. Pitts, *Chemistry of the Upper and Lower Atmosphere: Theory, Experiments and Applications*, Academic Press, San Diego, CA, 2000.
4 B. J. Finlayson-Pitts, *Res. Chem. Intermed.*, 1993, **19**, 235–249.
5 W. C. Keene, in *Naturally Produced Organohalogens*, ed. A. Grimvall and E. W. B. de Leer, Kluwer Academic Publishers, Dordrecht, 1995, pp. 363–373.
6 A. D. Keil and P. B. Shepson, *J. Geophys. Res.*, 2006, **111**, D17303.
7 P. J. Tackett, A. E. Cavender, A. D. Keil, P. B. Shepson, J. W. Bottenheim, S. Morin, J. Deary, A. Steffen and C. Doerge, *J. Geophys. Res.*, 2007, **112**, D07306.
8 S. Senkan, *Environ. Sci. Technol.*, 1988, **22**, 368–370.
9 W. Tsang, *Combust. Sci. Technol.*, 1990, **74**, 99–116.
10 M. Frenklach, *Combust. Sci. Technol.*, 1990, **74**, 283–296.
11 M. M. Tirtowidjojo, B. T. Colegrove and J. L. Durant, *Ind. Eng. Chem. Res.*, 1995, **34**, 4202–4211.
12 R. T. Morrison and R. N. Boyd, *Organic Chemistry*, Allyn and Bacon, Newton, MA, 1983.
13 T. H. Lowry and K. S. Richardson, *Mechanism and Theory in Organic Chemistry*, HarperCollins, New York, 1987.
14 M. L. Poutsma, *Science*, 1967, **157**, 997–1005.
15 F. Freeman, *Chem. Rev.*, 1975, **75**, 439–490.
16 R. J. Cvetanovic, *Adv. Photochem.*, 1963, **1**, 115–182.
17 C. A. Taatjes, *Int. Rev. Phys. Chem.*, 1999, **18**, 419–458.
18 J. A. Kerr and M. J. Parsonage, *Evaluated Kinetic Data on Gas Phase Addition Reactions: Reactions of Atoms and Radicals with Alkenes, Alkynes and Aromatic Compounds*, Butterworth, London, 1972.
19 P. Braña, B. Menéndez, T. Fernández and J. A. Sordo, *J. Phys. Chem. A*, 2000, **104**, 10842–10854.
20 P. Braña, B. Menéndez, T. Fernández and J. A. Sordo, *Chem. Phys. Lett.*, 2000, **325**, 693–697.
21 P. Braña and J. A. Sordo, *J. Am. Chem. Soc.*, 2001, **123**, 10348–10353.
22 P. Braña and J. A. Sordo, *J. Comput. Chem.*, 2003, **24**, 2044–2062.
23 *Vibrational Spectroscopy of Trapped Species*, ed. H. E. Hallam, Wiley, New York, 1973.
24 *Chemistry and Physics of Matrix-Isolated Species*, ed. L. Andrews and M. Moskovits, Elsevier, Amsterdam, 1989.
25 R. M. Romano, C. O. Della Védova and A. J. Downs, *Chem. Commun.*, 2001, 2638–2639.
26 Y. A. Tobón, L. I. Nieto, R. M. Romano, C. O. Della Védova and A. J. Downs, *J. Phys. Chem. A*, 2006, **110**, 2674–2681.
27 Y. A. Tobón, R. M. Romano, C. O. Della Védova and A. J. Downs, *Inorg. Chem.*, 2007, **46**, 4692–4703.
28 T. Momose and T. Shida, *Bull. Chem. Soc. Jpn.*, 1998, **71**, 1–15.
29 K. Yashioka, P. L. Raston and D. T. Anderson, *Int. Rev. Phys. Chem.*, 2006, **25**, 469–496.
30 J. V. Kranendonk, *Solid Hydrogen: Theory of the Properties of Solid H_2, HD, and D_2*, Plenum Press, New York, 1983.
31 I. F. Silvera, *Rev. Mod. Phys.*, 1980, **52**, 393–452.
32 T. Oka, *Annu. Rev. Phys. Chem.*, 1993, **44**, 299–333.
33 S. Tam, M. E. Fajardo, H. Katsuki, H. Hoshina, T. Wakabayashi and T. Momose, *J. Chem. Phys.*, 1999, **111**, 4191–4198.
34 T. Momose, H. Hoshina, M. Fushitani and H. Katsuki, *Vib. Spectrosc.*, 2004, **34**, 95–108.
35 Y.-P. Lee, Y.-J. Wu, R. M. Lees, L.-H. Xu and J. T. Hougen, *Science*, 2006, **311**, 365–368.
36 N. Sogoshi, T. Wakabayashi, T. Momose and T. Shida, *J. Phys. Chem. A*, 1997, **101**, 522–527.
37 Y.-J. Wu, X. Yang and Y.-P. Lee, *J. Chem. Phys.*, 2004, **120**, 1168–1171.
38 C.-W. Huang, Y.-C. Lee and L. Yuan-Pern, *J. Chem. Phys.*, 2010, **132**, 164303.
39 J. C. Amicangelo and Y.-P. Lee, *J. Phys. Chem. Lett.*, 2010, **1**, 2956–2961.
40 Y.-P. Lee, Y.-J. Wu and J. T. Hougen, *J. Chem. Phys.*, 2008, **129**, 104502.
41 P. L. Raston and D. T. Anderson, *Phys. Chem. Chem. Phys.*, 2006, **8**, 3124–3129.
42 C. Møller and M. S. Plesset, *Phys. Rev.*, 1934, **46**, 618–622.
43 D. E. Woon and T. H. Dunning, *J. Chem. Phys.*, 1993, **98**, 1358–1371.
44 A. D. Becke, *Phys. Rev. A*, 1988, **38**, 3098–3100.
45 A. D. Becke, *J. Chem. Phys.*, 1996, **104**, 1040–1046.
46 C. Lee, W. Yang and R. G. Parr, *Phys. Rev. B: Condens. Matter*, 1988, **37**, 785–789.
47 M. J. Frisch, G. W. Trucks, H. B. Schlegel, G. E. Scuseria, M. A. Robb, J. R. Cheeseman, J. A. Montgomery, Jr., T. Vreven, K. N. Kudin, J. C. Burant, J. M. Millam, S. S. Lyengar, J. Tomasi, V. Barone, B. Mennucci, M. Cossi, G. Scalmani, N. Rega, G. A. Petersson, H. Nakatsuji, M. Hada, M. Ehara, K. Toyota, R. Fukuda, J. Hasegawa, M. Ishida, T. Nakajima,

Y. Honda, O. Kitao, H. Nakai, M. Klene, X. Li, J. E. Knox, H. P. Hratchian, J. B. Cross, V. Bakken, C. Adamo, J. Jaramillo, R. Gomperts, R. E. Stratmann, O. Yazyev, A. J. Austin, R. Cammi, C. Pomelli, J. W. Ochterski, P. Y. Ayala, K. Morokuma, G. A. Voth, P. Salvador, J. J. Dannenberg, V. G. Zakrzewski, S. Dapprich, A. D. Daniels, M. C. Strain, O. Farkas, D. K. Malick, A. D. Rabuck, K. Raghavachari, J. B. Foresman, J. V. Ortiz, Q. Cui, A. G. Baboul, S. Clifford, J. Cioslowski, B. B. Stefanov, G. Liu, A. Liashenko, P. Piskorz, I. Komaromi, R. L. Martin, D. J. Fox, T. Keith, M. A. Al-Laham, C. Y. Peng, A. Nanayakkara, M. Challacombe, P. M. W. Gill, B. Johnson, W. Chen, M. W. Wong, C. Gonzalez and J. A. Pople, *GAUSSIAN 03*, Gaussian, Inc., Wallingford, CT, Revision D.01 edn, 2004.

48 T. Shimanouchi, *Tables of Molecular Vibrational Frequencies: Consolidated Volume I*, in *NIST Chemistry WebBook, Standard Reference Database Number 69*, ed. P. J. Linstrom and W. G. Mallard, National Institute of Standards and Technology, Gaithersburg, MD.

49 J. M. L. Martin, T. J. Lee, P. R. Taylor and J.-P. Francois, *J. Chem. Phys.*, 1995, **103**, 2589–2602.

50 L. Fredin and B. Nelander, *J. Mol. Struct.*, 1973, **16**, 205–216.

51 S. Holroyd, A. J. Barnes, S. Suzuki and W. J. Orville-Thomas, *J. Raman Spectrosc.*, 1982, **12**, 162–164.

52 S. Mizushima, T. Shimanouchi, I. Harada, Y. Abe and H. Takeuchi, *Can. J. Phys.*, 1975, **53**, 2085–2094.

53 S. C. Kettwich, P. L. Raston and D. T. Anderson, *J. Phys. Chem. A*, 2009, **113**, 7621–7629.

54 T. Kumada, S. Mori, T. Nagasaka, J. Kumagai and T. Miyazaki, *J. Low Temp. Phys.*, 2001, **122**, 265–277.

55 M. Fushitani and T. Momose, *J. Low Temp. Phys.*, 2003, **29**, 740–743.

56 D. T. Anderson, R. J. Hinde, S. Tam and M. E. Fajardo, *J. Chem. Phys.*, 2002, **116**, 594–607.

57 A. J. Barnes, *J. Mol. Struct.*, 1983, **100**, 259–280.

58 G. Chettur and A. Snelson, *J. Phys. Chem.*, 1987, **91**, 3483–3488.

59 J. Pacansky and B. Schrader, *J. Chem. Phys.*, 1983, **78**, 1033–1038.

60 P. L. Raston and D. T. Anderson, *J. Chem. Phys.*, 2007, **126**, 021106.

61 Y. Kurosaki, *J. Mol. Struct. (THEOCHEM)*, 2000, **503**, 231–240.

62 H. Y. Afeefy, J. F. Liebman and S. E. Stein, *Neutral Thermochemical Data*, in *NIST Chemistry WebBook, Standard Reference Database Number 69*, ed. P. J. Linstrom and W. G. Mallard, National Institute of Standards and Technology, Gaithersburg, MD.

63 NIST Chemical Kinetics Database, *NIST Standard Reference Database 17, Version 7.0 (Web Version), Release 1.6.1, Data Version 2011.06*, National Institute of Standards and Technology, Gaithersburg, MD.